

<sup>1</sup> **Critical transitions and the fragmenting of global forests**

<sup>2</sup> **Leonardo A. Saravia<sup>1 3</sup>, Santiago R. Doyle<sup>1</sup>, Benjamin Bond-Lamberty<sup>2</sup>**

<sup>3</sup> 1. Instituto de Ciencias, Universidad Nacional de General Sarmiento, J.M. Gutierrez 1159 (1613), Los  
<sup>4</sup> Polvorines, Buenos Aires, Argentina.

<sup>5</sup> 2. Pacific Northwest National Laboratory, Joint Global Change Research Institute at the University of  
<sup>6</sup> Maryland—College Park, 5825 University Research Court #3500, College Park, MD 20740, USA

<sup>7</sup> 3. Corresponding author e-mail: lsaravia@ungs.edu.ar

<sup>8</sup> **Keywords:** Forest fragmentation, early warning signals, percolation, power-laws, MODIS, critical transitions

<sup>9</sup> **Running title:** Critical fragmentation in global forest

<sup>10</sup> **Abstract**

<sup>11</sup> 1. Forests provide critical habitat for many species, essential ecosystem services, and are coupled to  
<sup>12</sup> atmospheric dynamics through exchanges of energy, water and gases. One of the most important  
<sup>13</sup> changes produced in the biosphere is the replacement of forest areas with human dominated landscapes.  
<sup>14</sup> This usually leads to fragmentation, altering the sizes of patches, the structure and function of the  
<sup>15</sup> forest. Here we studied the distribution and dynamics of forest patch sizes at a global level, examining  
<sup>16</sup> signals of a critical transition from an unfragmented to a fragmented state.

<sup>17</sup> 2. We used MODIS vegetation continuous field to estimate the forest patches at a global level and de-  
<sup>18</sup> fined wide regions of connected forest across continents and big islands. We search for critical phase  
<sup>19</sup> transitions, where the system state of the forest changes suddenly at a critical point in time; this  
<sup>20</sup> implies an abrupt change in connectivity that causes an increased fragmentation level. We studied the  
<sup>21</sup> distribution of forest patch sizes and the dynamics of the largest patch over the last fifteen years, as  
<sup>22</sup> the conditions that indicate that a region is near a critical fragmentation threshold are related to patch  
<sup>23</sup> size distribution and temporal fluctuations of the largest patch.

<sup>24</sup> 3. We found some necessary evidence that allows us to analyze fragmentation as a critical transition:  
<sup>25</sup> all regions followed a power-law distribution over the fifteen years. We also found that the Philip-  
<sup>26</sup> pines region probably went through a critical transition from a fragmented to an unfragmented state.  
<sup>27</sup> Neotropical regions with the highest deforestation rates—South America, Southeast Asia, Africa—all  
<sup>28</sup> met the criteria to be near a critical fragmentation threshold.

<sup>29</sup> 4. This implies that human pressures and climate forcings might trigger undesired effects of fragmentation,  
<sup>30</sup> such as species loss and degradation of ecosystems services, in these regions. The simple criteria  
<sup>31</sup> proposed here could be used as an early warning to estimate the distance to a fragmentation threshold  
<sup>32</sup> in forest around the globe and a predictor of a planetary tipping point.

### <sup>33</sup> Introduction

<sup>34</sup> Forests are one of the most important biomes on earth, providing habitat for a large proportion of species  
<sup>35</sup> and contributing extensively to global biodiversity (Crowther et al., 2015). In the previous century human  
<sup>36</sup> activities have influenced global bio-geochemical cycles (Bonan, 2008; Canfield, Glazer, & Falkowski, 2010),  
<sup>37</sup> with one of the most dramatic changes being the replacement of 40% of Earth's formerly biodiverse land  
<sup>38</sup> areas with landscapes that contain only a few species of crop plants, domestic animals and humans (J. A.  
<sup>39</sup> Foley et al., 2011). These local changes have accumulated over time and now constitute a global forcing  
<sup>40</sup> (Barnosky et al., 2012).

<sup>41</sup> Another global scale forcing that is tied to habitat destruction is fragmentation, which is defined as the  
<sup>42</sup> division of a continuous habitat into separated portions that are smaller and more isolated. Fragmentation  
<sup>43</sup> produces multiple interwoven effects: reductions of biodiversity between 13% and 75%, decreasing forest  
<sup>44</sup> biomass, and changes in nutrient cycling (Haddad et al., 2015). The effects of fragmentation are not only  
<sup>45</sup> important from an ecological point of view but also that of human activities, as ecosystem services are deeply  
<sup>46</sup> influenced by the level of landscape fragmentation (Angelsen, 2010; Mitchell et al., 2015; Rudel et al., 2005).

<sup>47</sup> Ecosystems have complex interactions between species and present feedbacks at different levels of organization  
<sup>48</sup> (Gilman, Urban, Tewksbury, Gilchrist, & Holt, 2010), and external forcings can produce abrupt changes  
<sup>49</sup> from one state to another, called critical transitions (Scheffer et al., 2009). These abrupt state shifts cannot  
<sup>50</sup> be linearly forecasted from past changes, and are thus difficult to predict and manage (Scheffer et al., 2009).  
<sup>51</sup> Such 'critical' transitions have been detected mostly at local scales (S. R. Carpenter et al., 2011; Drake &  
<sup>52</sup> Griffen, 2010), but the accumulation of changes in local communities that overlap geographically can propagate  
<sup>53</sup> and theoretically cause an abrupt change of the entire system at larger scales (Barnosky et al., 2012).  
<sup>54</sup> Coupled with the existence of global scale forcings, this implies the possibility that a critical transition could  
<sup>55</sup> occur at a global scale (C. Folke et al., 2011; Rockstrom et al., 2009).

<sup>56</sup> Complex systems can experience two general classes of critical transitions (R V Solé, 2011). In so-called first  
<sup>57</sup> order transitions, a catastrophic regime shift that is mostly irreversible occurs because of the existence of  
<sup>58</sup> alternative stable states (Scheffer et al., 2001). This class of transitions is suspected to be present in a variety  
<sup>59</sup> of ecosystems such as lakes, woodlands, coral reefs (Scheffer et al., 2001), semi-arid grasslands (Brandon T.  
<sup>60</sup> Bestelmeyer et al., 2011), and fish populations (Vasilakopoulos & Marshall, 2015). They can be the result of  
<sup>61</sup> positive feedback mechanisms (Villa Martín, Bonachela, Levin, & Muñoz, 2015); for example, fires in some  
<sup>62</sup> forest ecosystems were more likely to occur in previously burned areas than in unburned places (Kitzberger,  
<sup>63</sup> Aráoz, Gowda, Mermoz, & Morales, 2012).

64 The other class of critical transitions are continuous or second order transitions (Ricard V. Solé & Bascompte,  
65 2006). In these cases, there is a narrow region where the system suddenly changes from one domain to another,  
66 with the change being continuous and in theory reversible. This kind of transitions were suggested to be  
67 present in tropical forest (S. Pueyo et al., 2010), semi-arid mountain ecosystems (McKenzie & Kennedy,  
68 2012), tundra shrublands (Naito & Cairns, 2015). The transition happens at a critical point where we can  
69 observe a distinctive spatial pattern: scale invariant fractal structures characterized by power law patch  
70 distributions (Stauffer & Aharony, 1994).

71 There are several processes that can convert a catastrophic transition to a second order transitions (Villa  
72 Martín et al., 2015). These include stochasticity, such as demographic fluctuations, spatial heterogeneities,  
73 and/or dispersal limitation. All these components are present in forest around the globe (Filotas et al.,  
74 2014; Fung, O'Dwyer, Rahman, Fletcher, & Chisholm, 2016; Seidler & Plotkin, 2006), and thus continuous  
75 transitions might be more probable than catastrophic transitions. Moreover there is some evidence of recovery  
76 in some systems that supposedly suffered an irreversible transition produced by overgrazing (Brandon T  
77 Bestelmeyer, Duniway, James, Burkett, & Havstad, 2013; J. Y. Zhang, Wang, Zhao, Xie, & Zhang, 2005)  
78 and desertification (Allington & Valone, 2010).

79 The spatial phenomena observed in continuous critical transitions deal with connectivity, a fundamental  
80 property of general systems and ecosystems from forests (Ochoa-Quintero, Gardner, Rosa, de Barros Ferraz,  
81 & Sutherland, 2015) to marine ecosystems (Leibold & Norberg, 2004) and the whole biosphere (Lenton &  
82 Williams, 2013). When a system goes from a fragmented to a connected state we say that it percolates (R  
83 V Solé, 2011). Percolation implies that there is a path of connections that involves the whole system. Thus  
84 we can characterize two domains or phases: one dominated by short-range interactions where information  
85 cannot spread, and another in which long range interactions are possible and information can spread over  
86 the whole area. (The term “information” is used in a broad sense and can represent species dispersal or  
87 movement.)

88 Thus, there is a critical “percolation threshold” between the two phases, and the system could be driven close  
89 to or beyond this point by an external force; climate change and deforestation are the main forces that could  
90 be the drivers of such a phase change in contemporary forests (Bonan, 2008; Haddad et al., 2015). There  
91 are several applications of this concept in ecology: species' dispersal strategies are influenced by percolation  
92 thresholds in three-dimensional forest structure (Ricard V Solé, Bartumeus, & Gamarra, 2005), and it has  
93 been shown that species distributions also have percolation thresholds (He & Hubbell, 2003). This implies  
94 that pushing the system below the percolation threshold could produce a biodiversity collapse (J. Bascompte  
95 & Solé, 1996; Pardini, Bueno, Gardner, Prado, & Metzger, 2010; Ricard V. Solé, Alonso, & Saldaña, 2004);

96 conversely, being in a connected state (above the threshold) could accelerate the invasion of forest into prairie  
97 (Loehle, Li, & Sundell, 1996; Naito & Cairns, 2015).

98 One of the main challenges with systems that can experience critical transitions—of any kind—is that the  
99 value of the critical threshold is not known in advance. In addition, because near the critical point a small  
100 change can precipitate a state shift of the system, they are difficult to predict. Several methods have been  
101 developed to detect if a system is close to the critical point, e.g. a deceleration in recovery from perturbations,  
102 or an increase in variance in the spatial or temporal pattern (Boettiger & Hastings, 2012; S. R. Carpenter  
103 et al., 2011; Dai, Vorselen, Korolev, & Gore, 2012; Hastings & Wysham, 2010).

104 The existence of a critical transition between two states has been established for forest at global scale in  
105 different works (Hirota, Holmgren, Nes, & Scheffer (2011); Verbesselt et al. (2016); Staal, Dekker, Xu, &  
106 Nes (2016); Wuyts, Champneys, & House (2017)). It was not probed, but is generally believed, that this  
107 constitutes a first order catastrophic transition. The regions where forest can grow are not distributed  
108 homogeneously, there are demographic fluctuations in forest growth and disturbances produced by human  
109 activities. Due to new theoretical advances (Villa Martín, Bonachela, & Muñoz, 2014; Villa Martín et al.,  
110 2015) all these factors imply that if these were first order transitions they will be converted or observed as  
111 second order continuous transitions. From this basis we applied indices derived from second order transitions  
112 to global forest cover dynamics.

113 In this study, our objective is to look for evidence that forests around the globe are near continuous critical  
114 point that represent a fragmentation threshold. We use the framework of percolation to first evaluate if  
115 forest patch distribution at a continental scale is described by a power law distribution and then examine  
116 the fluctuations of the largest patch. The advantage of using data at a continental scale is that for very  
117 large systems the transitions are very sharp (R V Solé, 2011) and thus much easier to detect than at smaller  
118 scales, where noise can mask the signals of the transition.

## 119 Methods

### 120 Study areas definition

121 We analyzed mainland forests at a continental scale, covering the whole globe, by delimiting land areas with  
122 a near-contiguous forest cover, separated with each other by large non-forested areas. Using this criterion,  
123 we delimited the following forest regions. In America, three regions were defined: South America temperate  
124 forest (SAT), subtropical and tropical forest up to Mexico (SAST), and USA and Canada forest (NA). Europe

125 and North Asia were treated as one region (EUAS). The rest of the delimited regions were South-east Asia  
126 (SEAS), Africa (AF), and Australia (OC). We also included in the analysis islands larger than  $10^5\text{km}^2$ . The  
127 mainland region has the number 1 e.g. OC1, and the nearby islands have consecutive numeration (Appendix  
128 S4, figure S1-S6). We applied this criterion to delimit regions because we based our study on percolation  
129 theory that assumes some kind of connectivity in the study area (see below).

### 130 **Forest patch distribution**

131 We studied forest patch distribution in each defined area from 2000 to 2015 using the MODerate-resolution  
132 Imaging Spectroradiometer (MODIS) Vegetation Continuous Fields (VCF) Tree Cover dataset version 051  
133 (C. DiMiceli et al., 2015). This dataset is produced at a global level with a 231-m resolution, from 2000  
134 onwards on an annual basis. There are several definition of forest based on percent tree cover (J. O. Sexton  
135 et al., 2015); we choose a range from 20% to 30% threshold in 5% increments to convert the percentage  
136 tree cover to a binary image of forest and non-forest pixels. This range is centered in the definition used by  
137 the United Nations' International Geosphere-Biosphere Programme (Belward, 1996), and studies of global  
138 fragmentation (Haddad et al., 2015) and includes the range used in other studies of critical transitions (Xu  
139 et al., 2016). Using this range we try to avoid the errors produced by low discrimination of MODIS VCF  
140 between forest and dense herbaceous vegetation at low forest cover and the saturation of MODIS VCF in  
141 dense forests (J. O. Sexton et al., 2013). We repeat all the analysis for this set of thresholds, except in  
142 some specific cases described below. Patches of contiguous forest were determined in the binary image by  
143 grouping connected forest pixels using a neighborhood of 8 forest units (Moore neighborhood). The MODIS  
144 VCF product defines the percentage of tree cover by pixel, but does not discriminate the type of trees  
145 so besides natural forest it includes plantations of tree crops like rubber, oil palm, eucalyptus and other  
146 managed stands (M. Hansen et al., 2014).

### 147 **Percolation theory**

148 A more in-depth introduction to percolation theory can be found elsewhere (Stauffer & Aharony, 1994) and  
149 a review from an ecological point of view is available (B. Oborny, Szabó, & Meszéna, 2007). Here, to explain  
150 the basic elements of percolation theory we formulate a simple model: we represent our area of interest by a  
151 square lattice and each site of the lattice can be occupied—e.g. by forest—with a probability  $p$ . The lattice  
152 will be more occupied when  $p$  is greater, but the sites are randomly distributed. We are interested in the  
153 connection between sites, so we define a neighborhood as the eight adjacent sites surrounding any particular

site. The sites that are neighbors of other occupied sites define a patch. When there is a patch that connects the lattice from opposite sides, it is said that the system percolates. When  $p$  is increased from low values, a percolating patch suddenly appears at some value of  $p$  called the critical point  $p_c$ .

Thus percolation is characterized by two well defined phases: the unconnected phase when  $p < p_c$  (called subcritical in physics), in which species cannot travel far inside the forest, as it is fragmented; in a general sense, information cannot spread. The second is the connected phase when  $p > p_c$  (supercritical), species can move inside a forest patch from side to side of the area (lattice), i.e. information can spread over the whole area. Near the critical point several scaling laws arise: the structure of the patch that spans the area is fractal, the size distribution of the patches is power-law, and other quantities also follow power-law scaling (Stauffer & Aharony, 1994).

The value of the critical point  $p_c$  depends on the geometry of the lattice and on the definition of the neighborhood, but other power-law exponents only depend on the lattice dimension. Close to the critical point, the distribution of patch sizes is:

$$(1) \ n_s(p_c) \propto s^{-\alpha}$$

where  $n_s(p)$  is the number of patches of size  $s$ . The exponent  $\alpha$  does not depend on the details of the model and it is called universal (Stauffer & Aharony, 1994). These scaling laws can be applied for landscape structures that are approximately random, or at least only correlated over short distances (Gastner, Oborny, Zimmermann, & Pruessner, 2009). In physics this is called “isotropic percolation universality class”, and corresponds to an exponent  $\alpha = 2.05495$ . If we observe that the patch size distribution has another exponent it will not belong to this universality class and some other mechanism should be invoked to explain it. Percolation thresholds can also be generated by models that have some kind of memory (Hinrichsen, 2000; Ódor, 2004): for example, a patch that has been exploited for many years will recover differently than a recently deforested forest patch. In this case, the system could belong to a different universality class, or in some cases there is no universality, in which case the value of  $\alpha$  will depend on the parameters and details of the model (Corrado, Cherubini, & Pennetta, 2014).

To illustrate these concepts, we conducted simulations with a simple forest model with only two states: forest and non-forest. This type of model is called a “contact process” and was introduced for epidemics (Harris, 1974), but has many applications in ecology (Gastner et al., 2009; Ricard V. Solé & Bascompte, 2006). A site with forest can become extinct with probability  $e$ , and produce another forest site in a neighborhood with probability  $c$ . We use a neighborhood defined by an isotropic power law probability distribution. We defined a single control parameter as  $\lambda = c/e$  and ran simulations for the subcritical fragmentation state

185  $\lambda < \lambda_c$ , with  $\lambda = 2$ , near the critical point for  $\lambda = 2.5$ , and for the supercritical state with  $\lambda = 5$  (see  
186 supplementary data, gif animations).

187 **Patch size distributions**

188 We fitted the empirical distribution of forest patches calculated for each of the thresholds on the range  
189 we previously mentioned. We used maximum likelihood (Clauset, Shalizi, & Newman, 2009; Goldstein,  
190 Morris, & Yen, 2004) to fit four distributions: power-law, power-law with exponential cut-off, log-normal,  
191 and exponential. We assumed that the patch size distribution is a continuous variable that was discretized  
192 by remote sensing data acquisition procedure.

193 We set a minimal patch size ( $X_{min}$ ) at nine pixels to fit the patch size distributions to avoid artifacts at patch  
194 edges due to discretization (Weerman et al., 2012). Besides this hard  $X_{min}$  limit we set due to discretization,  
195 the power-law distribution needs a lower bound for its scaling behavior. This lower bound is also estimated  
196 from the data by maximizing the Kolmogorov-Smirnov (KS) statistic, computed by comparing the empirical  
197 and fitted cumulative distribution functions (Clauset et al., 2009). For the log-normal model we constrain  
198 the values of the  $\mu$  parameter to positive values, this parameter controls the mode of the distribution and  
199 when is negative most of the probability density of the distribution lies outside the range of the forest patch  
200 size data (Limpert, Stahel, & Abbt, 2001).

201 To select the best model we calculated corrected Akaike Information Criteria ( $AIC_c$ ) and Akaike weights for  
202 each model (Burnham & Anderson, 2002). Akaike weights ( $w_i$ ) are the weight of evidence in favor of model  
203  $i$  being the actual best model given that one of the  $N$  models must be the best model for that set of  $N$   
204 models. Additionally, we computed a likelihood ratio test (Clauset et al., 2009; Vuong, 1989) of the power  
205 law model against the other distributions. We calculated bootstrapped 95% confidence intervals (Crawley,  
206 2012) for the parameters of the best model; using the bias-corrected and accelerated (BCa) bootstrap (Efron  
207 & Tibshirani, 1994) with 10000 replications.

208 **Largest patch dynamics**

209 The largest patch is the one that connects the highest number of sites in the area. This has been used  
210 extensively to indicate fragmentation (R. H. Gardner & Urban, 2007; Ochoa-Quintero et al., 2015). The  
211 relation of the size of the largest patch  $S_{max}$  to critical transitions has been extensively studied in relation  
212 to percolation phenomena (Bazant, 2000; Botet & Ploszajczak, 2004; Stauffer & Aharony, 1994), but seldom  
213 used in ecological studies (for an exception see Gastner et al. (2009)). When the system is in a connected

214 state ( $p > p_c$ ) the landscape is almost insensitive to the loss of a small fraction of forest, but close to the  
215 critical point a minor loss can have important effects (B. Oborny et al., 2007; Ricard V. Solé & Bascompte,  
216 2006), because at this point the largest patch will have a filamentary structure, i.e. extended forest areas  
217 will be connected by thin threads. Small losses can thus produce large fluctuations.

218 One way to evaluate the fragmentation of the forest is to calculate the proportion of the largest patch  
219 against the total area (T. H. Keitt, Urban, & Milne, 1997). The total area of the regions we are considering  
220 (Appendix S4, figures S1-S6) may not be the same than the total area that the forest could potentially  
221 occupy, thus a more accurate way to evaluate the weight of  $S_{max}$  is to use the total forest area, that can  
222 be easily calculated summing all the forest pixels. We calculate the proportion of the largest patch for each  
223 year, dividing  $S_{max}$  by the total forest area of the same year:  $RS_{max} = S_{max} / \sum_i S_i$ . This has the effect of  
224 reducing the  $S_{max}$  fluctuations produced due to environmental or climatic changes influences in total forest  
225 area. When the proportion  $RS_{max}$  is large (more than 60%) the largest patch contains most of the forest  
226 so there are fewer small forest patches and the system is probably in a connected phase. Conversely, when  
227 it is low (less than 20%), the system is probably in a fragmented phase (Saravia & Momo, 2017). As we  
228 calculated these largest patch indices for different thresholds, the values of the total forest area and the value  
229 of  $S_{max}$  are lower as threshold is higher, we expect that the value of  $RS_{max}$  will change and probably be  
230 lower at high thresholds. To define if a region will be in a connected or unconnected state we used the  $RS_{max}$   
231 of the highest threshold (40%) which is more conservative to evaluate the risk of fragmentation and includes  
232 the most dense forest area. Additionally if  $RS_{max}$  is a good indicator of the fragmented or unfragmented  
233 state of the forest and these are the two alternative states for the critical transition the  $RS_{max}$  distribution  
234 of frequencies should be bimodal (Brandon T. Bestelmeyer et al., 2011); so we apply the Hartigan's dip test  
235 that measures departures from unimodality (J. A. Hartigan & Hartigan, 1985).

236 The  $RS_{max}$  is a useful qualitative index that does not tell us if the system is near or far from the critical  
237 transition; this can be evaluated using the temporal fluctuations. We calculate the fluctuations around the  
238 mean with the absolute values  $\Delta S_{max} = S_{max}(t) - \langle S_{max} \rangle$ , using the proportions of  $RS_{max}$ . To characterize  
239 fluctuations we fitted three empirical distributions: power-law, log-normal, and exponential, using the same  
240 methods described previously. We expect that large fluctuation near a critical point have heavy tails (log-  
241 normal or power-law) and that fluctuations far from a critical point have exponential tails, corresponding to  
242 Gaussian processes (Rooij, Nash, Rajaraman, & Holden, 2013). As the data set spans 16 years, it is probable  
243 that will do not have enough power to reliably detect which distribution is better (Clauset et al., 2009). To  
244 improve this we used the same likelihood ratio test we used previously (Clauset et al., 2009; Vuong, 1989);  
245 if the p-value obtained to compare the best distribution against the others we concluded that there is not

246 enough data to decide which is the best model. We generated animated maps showing the fluctuations of  
247 the two largest patches at 30% threshold, to aid in the interpretations of the results.

248 A robust way to detect if the system is near a critical transition is to analyze the increase in variance of  
249 the density (Benedetti-Cecchi, Tamburello, Maggi, & Bulleri, 2015). It has been demonstrated that the  
250 variance increase in density appears when the system is very close to the transition (Corrado et al., 2014),  
251 thus practically it does not constitute an early warning indicator. An alternative is to analyze the variance of  
252 the fluctuations of the largest patch  $\Delta S_{max}$ : the maximum is attained at the critical point but a significant  
253 increase occurs well before the system reaches the critical point (Corrado et al., 2014; Saravia & Momo,  
254 2017). In addition, before the critical fragmentation, the skewness of the distribution of  $\Delta S_{max}$  should be  
255 negative, implying that fluctuations below the average are more frequent. We characterized the increase in  
256 the variance using quantile regression: if variance is increasing the slopes of upper or/and lower quartiles  
257 should be positive or negative.

258 All statistical analyses were performed using the GNU R version 3.3.0 (R Core Team, 2015), to fit the  
259 distributions of patch sizes we used the Python package powerlaw (Alstott, Bullmore, & Plenz, 2014). For  
260 the quantile regressions we used the R package quantreg (Koenker, 2016). Image processing was done  
261 in MATLAB r2015b (The Mathworks Inc.). The complete source code for image processing and statistical  
262 analysis, and the patch size data files are available at figshare <http://dx.doi.org/10.6084/m9.figshare.4263905>.

## 263 Results

264 The figure 1 shows an example of the distribution of the biggest 200 patches for years 2000 and 2014, this  
265 distribution is highly variable, but the biggest patch usually maintains its place. Sometimes the biggest  
266 patch breaks and then big fluctuations in its size are observed, as we will analyze below. Smaller patches  
267 can merge or break more easily so they enter or leave the list of 200, and this is why there is a color change  
268 across years.

269 The power law distribution was selected as the best model in 99% of the cases (Figure S7). In a small  
270 number of cases (1%) the power law with exponential cutoff was selected, but the value of the parameter  $\alpha$   
271 was similar by  $\pm 0.03$  to the pure power law (Table S1, and model fit data table). Additionally the patch size  
272 where the exponential tail begins is very large, thus we used the power law parameters for this cases (region  
273 EUAS3,SAST2). In finite-size systems the favored model should be the power law with exponential cut-off,  
274 because the power-law tails are truncated to the size of the system (Stauffer & Aharony, 1994). This implies  
275 that differences between the two kinds of power law models should be small. We observed that phenomena:

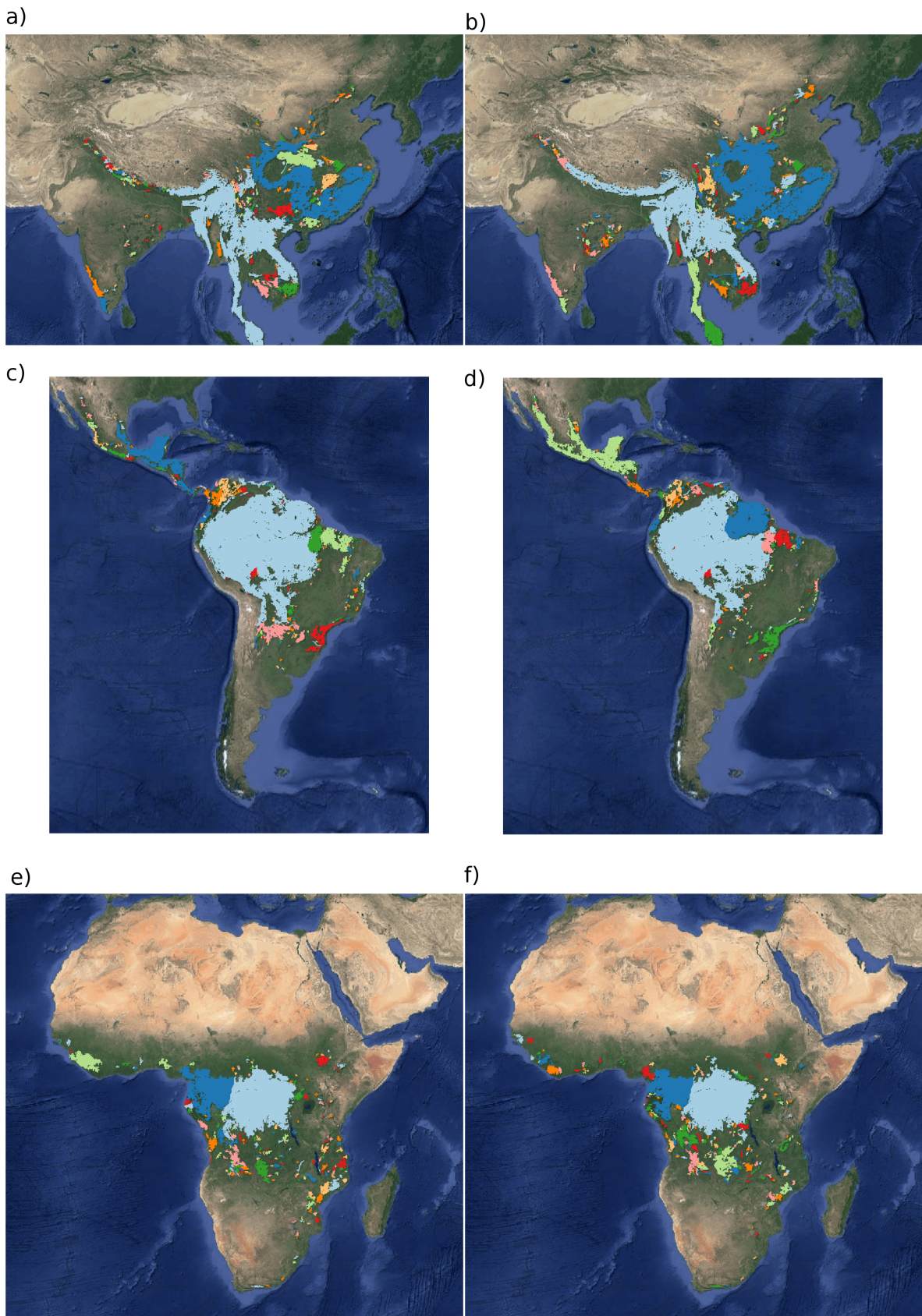


Figure 1: Forest patch distributions for continental regions for the years 2000 and 2014. The images are the 200 biggest patches, showed at a coarse pixel scale of 2.5 km. The regions are: a) & b) southeast Asia; c) & d) South America subtropical and tropical and e) & f) Africa mainland, for the years 2000 and 2014 respectively. The color palette was chosen to discriminate different patches and do not represent patch size.

276 when the pure power-law model is selected as the best model the likelihood ratio test shows that in 64% of  
277 the cases the differences with power law with exponential cutoff are not significant (p-value>0.05); in these  
278 cases the differences between the fitted  $\alpha$  for both models are less than 0.001. Instead the likelihood ratio  
279 test clearly differentiates the power law model from the exponential model (100% cases p-value<0.05), and  
280 the log-normal model (90% cases p-value<0.05).

281 The global mean of the power-law exponent  $\alpha$  is 1.967 and the bootstrapped 95% confidence interval is 1.964  
282 - 1.970. Besides that, the global values for each threshold are different, because their confidence intervals  
283 do not overlap, and their range goes from 1.90 to 2.01 (Table S1). Analyzing the biggest regions (Figure  
284 1, Table S2) the north hemisphere (EUAS1 & NA1) have similar values of  $\alpha$  (1.97, 1.98), pantropical areas  
285 have different  $\alpha$  with greatest values for South America (SAST1, 2.01) and in descending order Africa (AF1,  
286 1.946) and Southeast Asia (SEAS1, 1.895). With greater  $\alpha$  the fluctuations of patch sizes are lower and vice  
287 versa (M. E. J. Newman, 2005).

288 We calculated the total areas of forest and the largest patch  $S_{max}$  by year for different thresholds; as expected  
289 these two values increase for smaller thresholds (Table S3). We expect less variations in the largest patch  
290 relative to total forest area  $RS_{max}$  (Figure S9); in ten cases it keeps near or higher than 60% (EUAS2, NA5,  
291 OC2, OC3, OC4, OC5, OC6, OC8, SAST1, SAT1) over the 25-35 range or more. In four cases it keeps  
292 around 40% or less at least over the 25-30% range (AF1, EUAS3, OC1, SAST2) and in six cases there is  
293 a crossover from more than 60% to around 40% or less (AF2, EUAS1, NA1, OC7, SEAS1, SEAS2). This  
294 confirms the criteria of using the most conservative threshold value of 40% to interpret  $RS_{max}$  with regard  
295 to the fragmentation state of the forest. The frequency of  $RS_{max}$  showed bimodality (Figure 3) and the dip  
296 test rejected unimodality ( $D = 0.0416$ , p-value = 0.0003), which also indicates  $RS_{max}$  as a good index to  
297 study the fragmentation state of the forest.

298 The  $RS_{max}$  for regions with more than  $10^7$  km<sup>2</sup> of forest is shown in figure 4. South America tropical and  
299 subtropical (SAST1) is the only region with an average close to 60%, the other regions are below 30%. Eurasia  
300 mainland (EUAS1) has the lowest value near 20%. For regions with less total forest area (Figure S10, Table  
301 S3), Great Britain (EUAS3) has the lowest proportion less than 5%, Java (OC7) and Cuba (SAST2) are  
302 under 25%, while other regions such as New Guinea (OC2), Malaysia/Kalimantan (OC3), Sumatra (OC4),  
303 Sulawesi (OC5) and South New Zealand (OC6) have a very high proportion (75% or more). Philippines  
304 (SEAS2) seems to be a very interesting case because it seems to be under 30% until the year 2007, fluctuates  
305 around 30% in years 2008-2010, then jumps near 60% in 2011-2013 and then falls again to 30%, this seems  
306 an example of a transition from a fragmented state to a unfragmented one (figure S10).

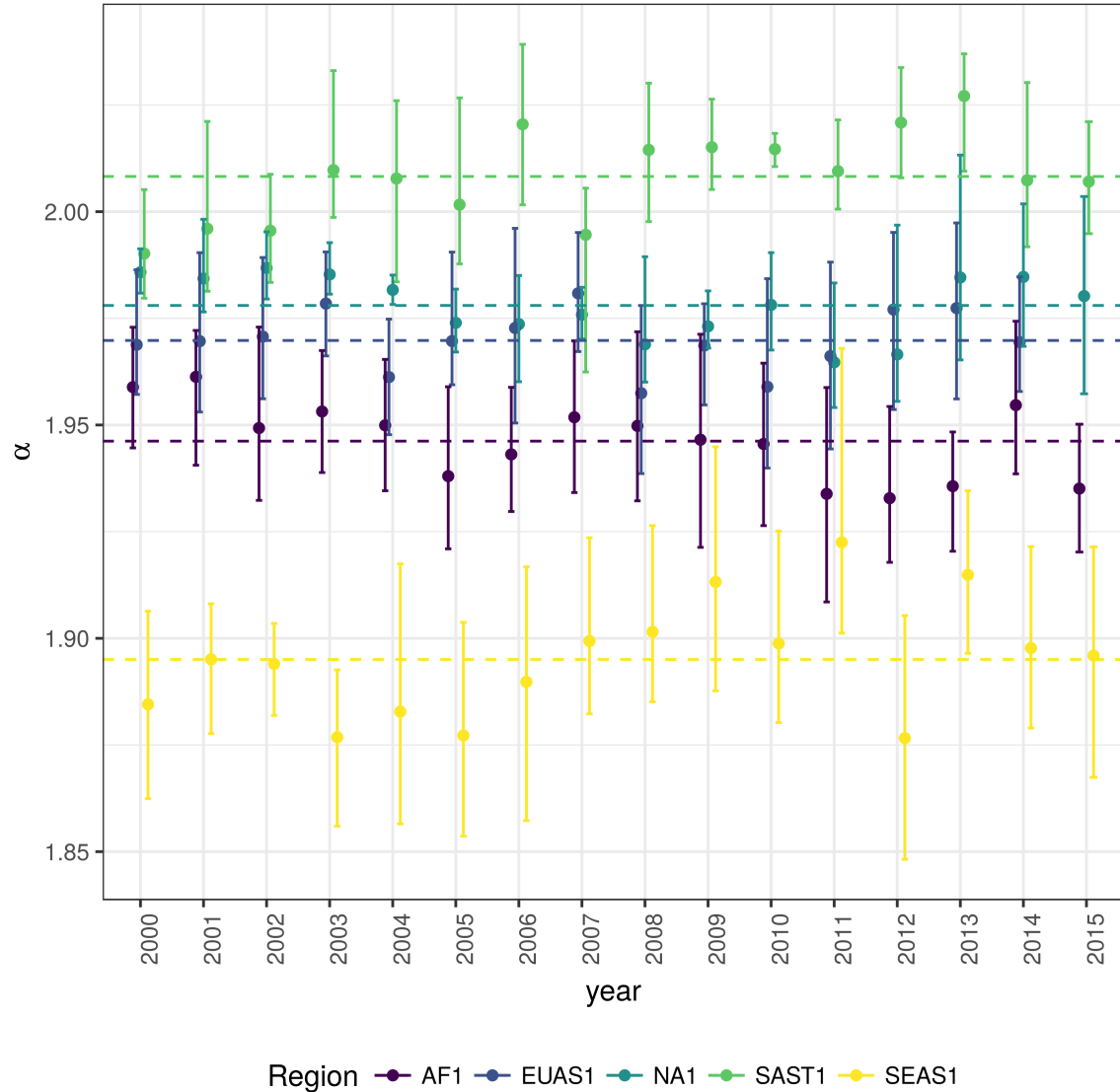


Figure 2: Power law exponents ( $\alpha$ ) of forest patch distributions for regions with total forest area  $> 10^7 \text{ km}^2$ . Dashed horizontal lines are the means by region, with 95% confidence interval error bars estimated by bootstrap resampling. The regions are AF1: Africa mainland, EUAS1: Eurasia mainland, NA1: North America mainland, SAST1: South America subtropical and tropical, SEAS1: Southeast Asia mainland.

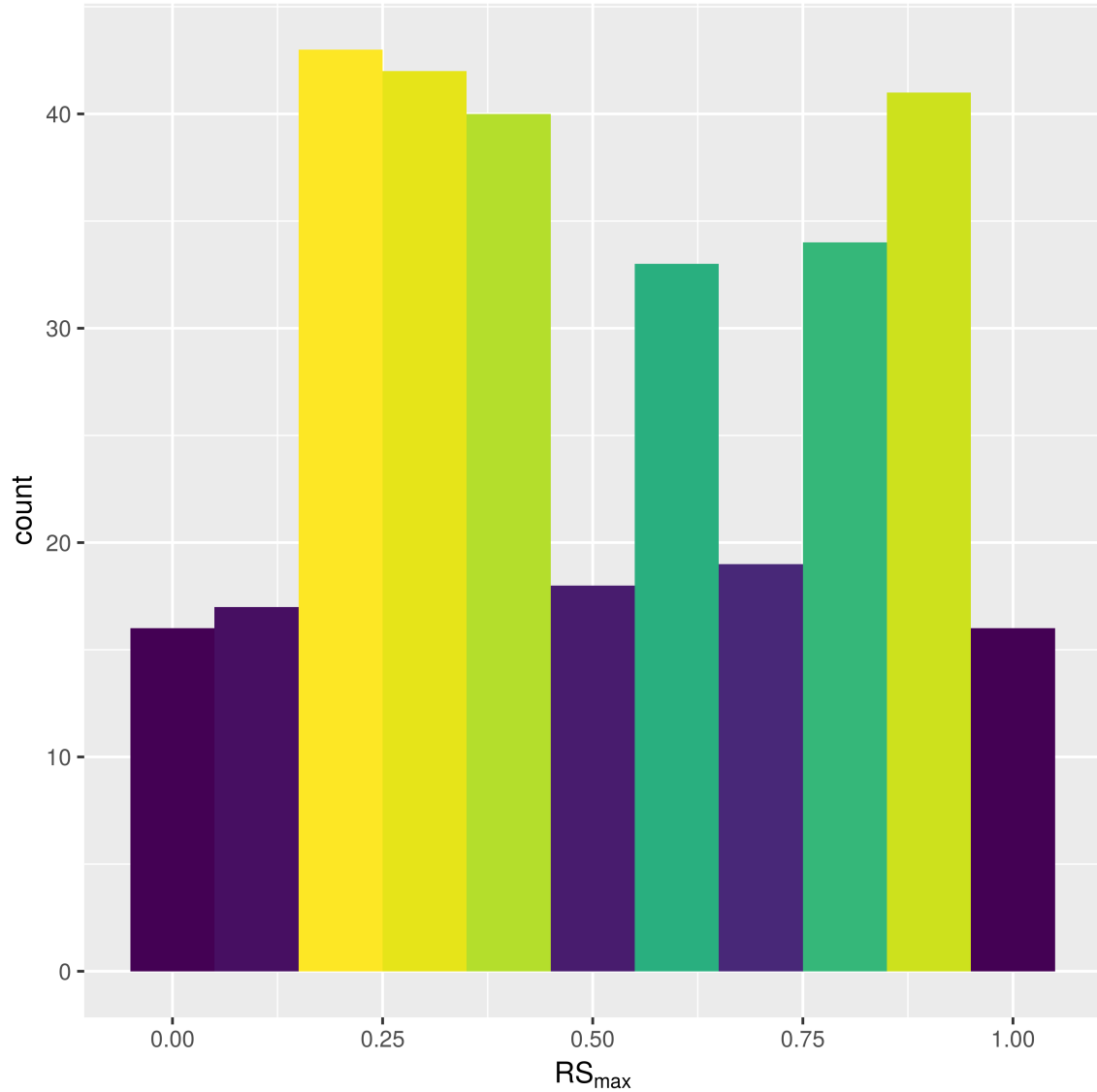


Figure 3: Frequency distribution of Largest patch proportion relative to total forest area  $RS_{max}$  calculated using a threshold of 40% of forest in each pixel to determine patches. Bimodality is observed and confirmed by the dip test ( $D = 0.0416$ ,  $p\text{-value} = 0.0003$ ). This indicates the existence of two states needed for a critical transition.

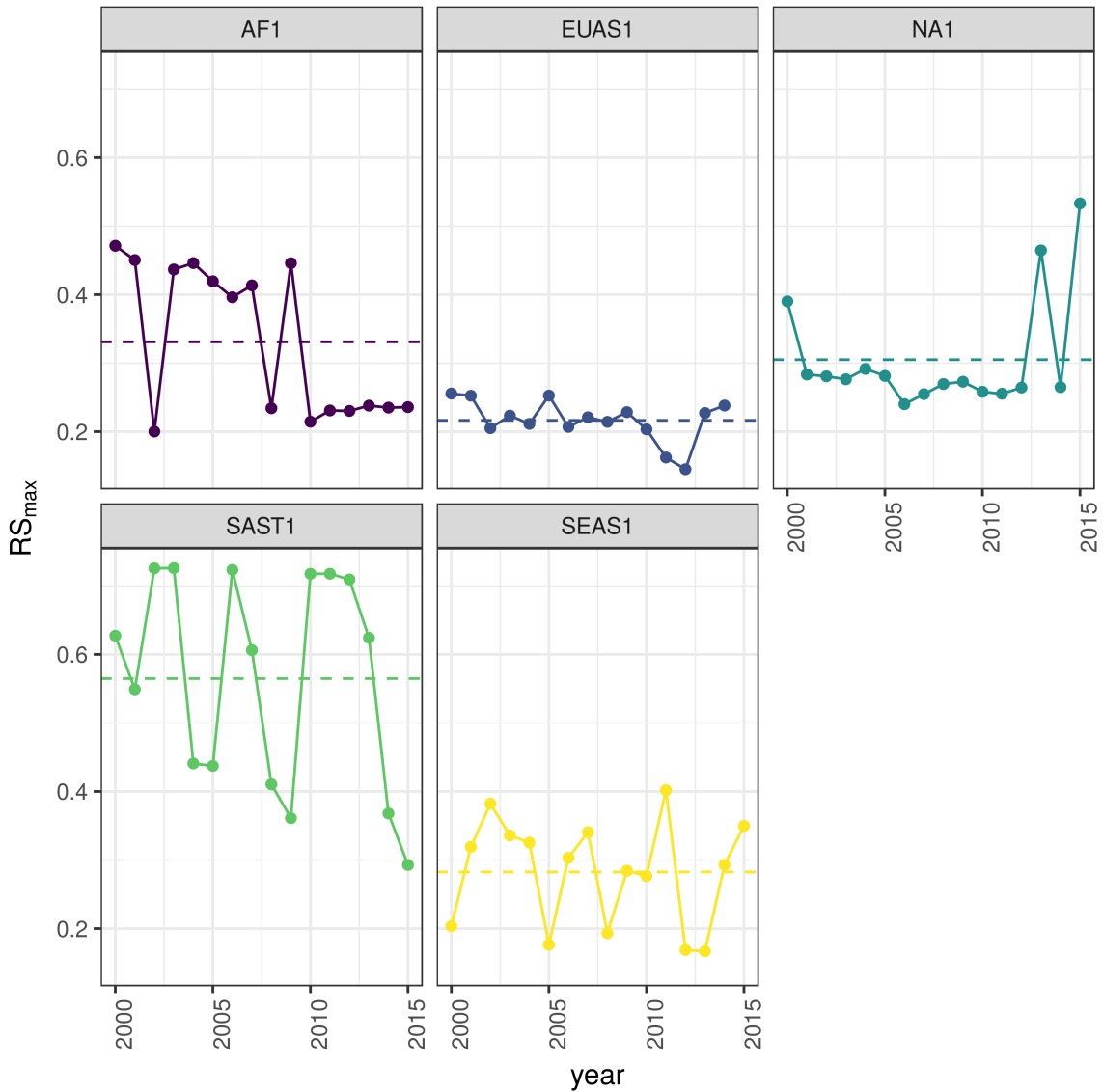


Figure 4: Largest patch proportion relative to total forest area  $RS_{max}$ , for regions with total forest area  $> 10^7 \text{ km}^2$ . We show here the  $RS_{max}$  calculated using a threshold of 40% of forest in each pixel to determine patches. Dashed lines are averages across time. The regions are AF1: Africa mainland, EUAS1: Eurasia mainland, NA1: North America mainland, SAST1: South America tropical and subtropical, SEAS1: Southeast Asia mainland.

307 We analyzed the distributions of fluctuations of the largest patch relative to total forest area  $\Delta RS_{max}$  and  
308 the fluctuations of the largest patch  $\Delta S_{max}$ . Besides the Akaike criteria identified different distributions as  
309 the best, in most cases the Likelihood ratio test is not significant thus the data is not enough to determine  
310 with confidence which is the best distribution. Only 1 case the distribution selected by the Akaike criteria is  
311 confirmed as the correct model for relative and absolute fluctuations (Table S4). Thus we do not apply this  
312 criteria because is not informative, we can not decide with reliability if the best distribution is the selected  
313 one.

314 The animations of the two largest patches (see supplementary data, largest patch gif animations) qualitatively  
315 shows the nature of fluctuations and if the state of the forest is connected or not. If the largest patch is  
316 always the same patch over time, the forest is probably not fragmented; this happens for regions with  $RS_{max}$   
317 of more than 40% such as AF2 (Madagascar), EUAS2 (Japan), NA5 (Newfoundland) and OC3 (Malaysia).  
318 In the regions with  $RS_{max}$  between 40% and 30% the identity of the largest patch could change or stay the  
319 same in time. For OC7 (Java) the largest patch changes and for AF1 (Africa mainland) it stays the same.  
320 Only for EUAS1 (Eurasia mainland) we observed that the two largest patches are always the same, implying  
321 that this region is probably composed of two independent domains and should be divided in further studies.  
322 The regions with  $RS_{max}$  less than 25%: SAST2 (Cuba) and EUAS3 (Great Britain), the largest patch always  
323 changes reflecting their fragmented state. In the case of SEAS2 (Philippines) a transition is observed, with  
324 the identity of the largest patch first variable, and then constant after 2010.

325 The results of quantile regressions are almost identical for  $\Delta RS_{max}$  and  $\Delta S_{max}$  (table S5); in very few cases  
326 only one of them is significant but we only take into account results where both are significant. Among the  
327 biggest regions, Africa (AF1) has a similar pattern across thresholds but only at 30% threshold is significant;  
328 the upper and lower quantiles have significant negative slopes, but the lower quantile slope is lower, implying  
329 that negative fluctuations and variance are increasing (Figure 5). Eurasia mainland (EUAS1) has significant  
330 slopes at 20%, 30% and 40% thresholds but the patterns are different at 20% variance is decreasing, at 30%  
331 and 40% only is increasing. This is because the largest patch is composed of pixels with different cover  
332 of forest, thus there are more variation in pixels from 30% to 20% than from 20% to less than 20%, then  
333 the fluctuations are happening between 40% and 20%. The signal is that the variation of the most dense  
334 portion of the largest patch is increasing withing a limited range. North America mainland (NA1) exhibits  
335 the same pattern at 20%, 25% and 30% thresholds: a significant lower quantile with positive slope, implying  
336 decreasing variance. South America tropical and subtropical (SAST1) have significant lower quantile with  
337 negative slope at 25% and 30% thresholds indicating an increase in variance. Finally, SEAS1 have a upper  
338 quantile with positive slope significant for 25% threshold, also indicating an increasing variance. The other

<sup>339</sup> regions, with forest area smaller than  $10^7 \text{ km}^2$  are showed in figure S11 and table S5. Philippines (SEAS2)  
<sup>340</sup> is an interesting case: the slopes of lower quantils are positive for thresholds 20% and 25%, and the upper  
<sup>341</sup> quantil slopes are positive for thresholds 30% and 40%; thus variance is decreasing at 20%-25% and increasing  
<sup>342</sup> at 30%-40%.

<sup>343</sup> The conditions that indicate that a region is near a critical fragmentation threshold are that patch size  
<sup>344</sup> distributions follow a power law; variance of  $\Delta RS_{max}$  is increasing in time; and skewness is negative. All  
<sup>345</sup> these conditions must happen at the same time at least for one threshold. When the threshold is higher more  
<sup>346</sup> dense regions of the forest are at risk. This happens for Africa mainland (AF1), Eurasia mainland(EUAS1),  
<sup>347</sup> Japan (EUAS2), Australia mainland (OC1), Malaysia/Kalimantan (OC3), Sumatra (OC4), South America  
<sup>348</sup> tropical & subtropical (SAST1), Cuba (SAST2), Southeast Asia, Mainland (SEAS1).

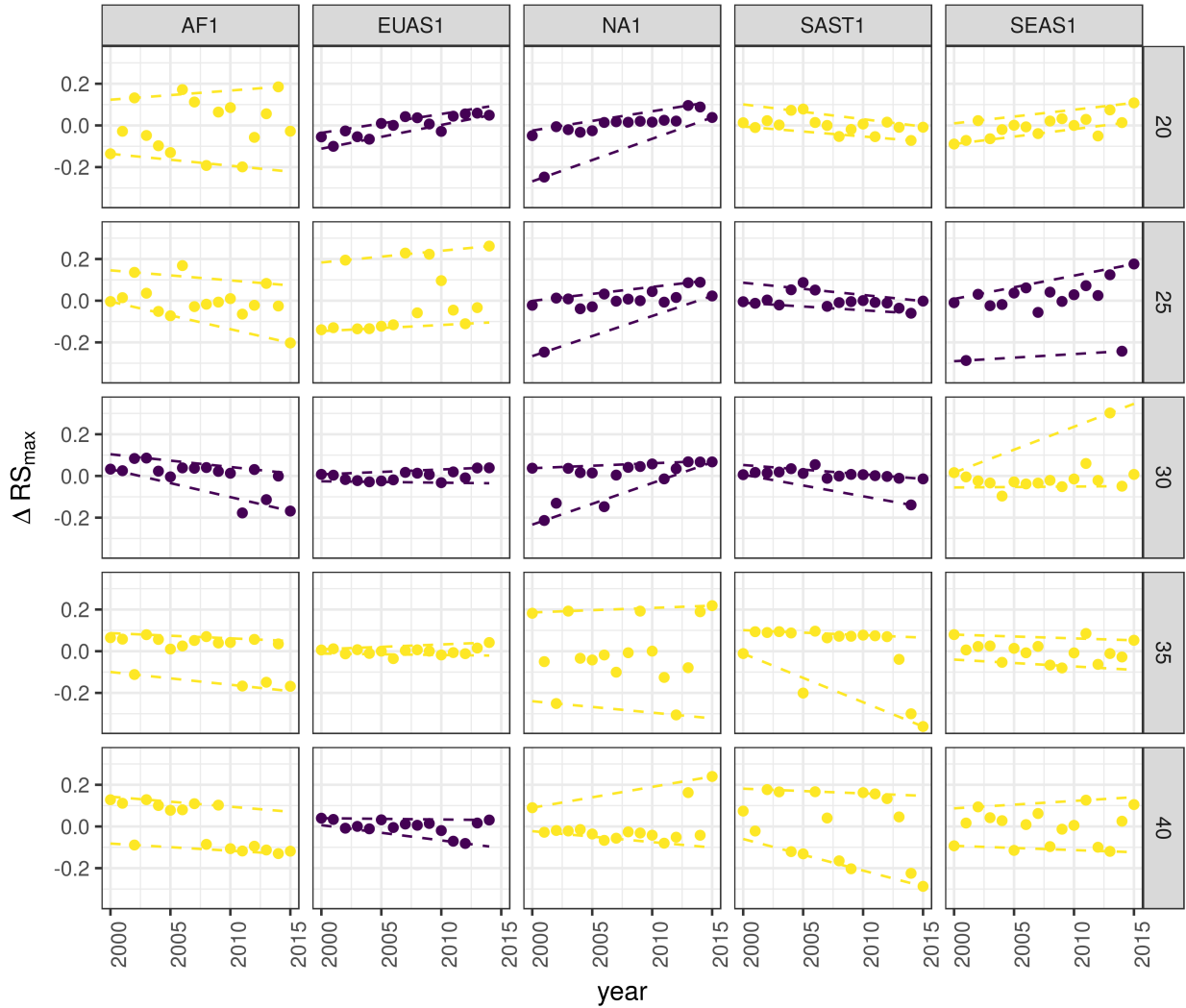


Figure 5: Largest patch fluctuations for regions with total forest area  $> 10^7 \text{ km}^2$  across years. The patch sizes are relative to the total forest area of the same year. Dashed lines are 90% and 10% quantile regressions, to show if fluctuations were increasing; purple (dark) panels have significant slopes. The regions are AF1: Africa mainland, EUAS1: Eurasia mainland, NA1: North America mainland, SAST1: South America tropical and subtropical, SEAS1: Southeast Asia mainland.

Table 1: Regions and indicators of closeness to a critical fragmentation point. Where:  $RS_{max}$  is the largest patch divided by the total forest area; Threshold is the value used to calculate patches from the MODIS VCF pixels;  $\Delta RS_{max}$  are the fluctuations of  $RS_{max}$  around the mean and the increase or decrease in the variance was estimated using quantile regressions; skewness was calculated for  $RS_{max}$ . NS means the results were non-significant. The conditions that determine the closeness to a fragmentation point are: increasing variance of  $\Delta RS_{max}$  and negative skewness.  $RS_{max}$  indicates if the forest is unfragmented ( $>0.6$ ) or fragmented ( $<0.3$ ).

| Region | Description                                    | $RS_{max}$ | Threshold | Variance of $\Delta RS_{max}$ | Skewness |
|--------|--|------------|-----------|-------------------------------|----------|
| AF1    | Africa mainland                                | 0.33       | 30        | Increase                      | -1.4653  |
| AF2    | Madagascar                                     | 0.48       | 20        | Increase                      | 0.7226   |
| EUAS1  | Eurasia, mainland                              | 0.22       | 20        | Decrease                      | -0.4814  |
| EUAS1  |  |            | 30        | Increase                      | 0.3113   |
| EUAS1  |  |            | 40        | Increase                      | -1.2790  |
| EUAS2  | Japan  | 0.94       | 35        | Increase                      | -0.3913  |
| EUAS2  |  |            | 40        | Increase                      | -0.5030  |
| EUAS3  | Great Britain                                  | 0.03       | 40        | NS                            |          |
| NA1    | North America, mainland                        | 0.31       | 20        | Decrease                      | -2.2895  |
| NA1    |  |            | 25        | Decrease                      | -2.4465  |
| NA1    |  |            | 30        | Decrease                      | -1.6340  |
| NA5    | Newfoundland                                   | 0.54       | 40        | NS                            |          |
| OC1    | Australia, Mainland                            | 0.36       | 30        | Increase                      | 0.0920   |
| OC1    |  |            | 35        | Increase                      | -0.8033  |
| OC2    | New Guinea                                     | 0.96       | 25        | Decrease                      | -0.1003  |
| OC2    |  |            | 30        | Decrease                      | 0.1214   |
| OC2    |  |            | 35        | Decrease                      | -0.0124  |
| OC3    | Malaysia/Kalimantan                            | 0.92       | 35        | Increase                      | -1.0147  |
| OC3    |  |            | 40        | Increase                      | -1.5649  |
| OC4    | Sumatra  | 0.84       | 20        | Increase                      | -1.3846  |
| OC4    |  |            | 25        | Increase                      | -0.5887  |
| OC4    |  |            | 30        | Increase                      | -1.4226  |
| OC5    | Sulawesi                                       | 0.82       | 40        | NS                            |          |
| OC6    | New Zealand South Island                       | 0.75       | 40        | Increase                      | 0.3553   |
| OC7    | Java   | 0.16       | 40        | NS                            |          |
| OC8    | New Zealand North Island                       | 0.64       | 40        | NS                            |          |
| SAST1  | South America, Tropical and Subtropical forest | 0.56       | 25        | Increase                      | 1.0519   |
| SAST1  |  |            | 30        | Increase                      | -2.7216  |
| SAST2  | Cuba   | 0.15       | 20        | Increase                      | 0.5049   |
| SAST2  |  |            | 25        | Increase                      | 1.7263   |
| SAST2  |  |            | 30        | Increase                      | 0.1665   |
| SAST2  |  |            | 40        | Increase                      | -0.5401  |
| SAT1   | South America, Temperate forest                | 0.54       | 25        | Decrease                      | 0.1483   |
| SAT1   |  |            | 30        | Decrease                      | -1.6059  |
| SAT1   |  |            | 35        | Decrease                      | -1.3809  |
| SEAS1  | Southeast Asia, Mainland                       | 0.28       | 25        | Increase                      | -1.3328  |
| SEAS2  | Philippines                                    | 0.33       | 20        | Decrease                      | -1.6373  |
| SEAS2  |  |            | 25        | Decrease                      | -0.6648  |
| SEAS2  |  |            | 30        | Increase                      | 0.1517   |

| Region | Description | $RS_{max}$ | Threshold | Variance of $\Delta RS_{max}$ | Skewness |
|--------|-------------|------------|-----------|-------------------------------|----------|
| SEAS2  |             |            | 40        | Increase                      | 1.5996   |

## 349 Discussion

350 We found that the forest patch distribution of all regions of the world followed power laws spanning seven  
 351 orders of magnitude. These include tropical rainforest, boreal and temperate forest. Power laws have  
 352 previously been found for several kinds of vegetation, but never at global scales as in this study. Moreover  
 353 the range of the estimated power law exponents is relatively narrow besides we used different thresholds  
 354 (1.90 - 2.01). This suggest the existence of one unifying mechanism or different mechanism that act in the  
 355 same way in different regions.

356 Several mechanisms have been proposed for the emergence of power laws in forest: the first is related self  
 357 organized criticality (SOC), when the system is driven by its internal dynamics to a critical state; this has  
 358 been suggested mainly for fire-driven forests (Hantson, Pueyo, & Chuvieco, 2015; Zinck & Grimm, 2009).  
 359 Real ecosystems do not seem to meet the requirements of SOC dynamics because their are driven both  
 360 endogenous and exogenous controls, non-homogeneous and they may not have the separation of time scales  
 361 [Ricard V Solé, Alonso, & Mckane (2002);Sole2006]; furthermore there is some evidence that these conditions  
 362 are not meet (McKenzie & Kennedy, 2012; S. Pueyo et al., 2010). A second possible mechanism, suggested  
 363 by Pueyo et al. (2010), is isotropic percolation, when a system is near the critical point power law structures  
 364 arise. This is equivalent to the random forest model that we explained previously, and requires the tuning  
 365 of an external environmental condition to carry the system to this point. We did not expect forest growth  
 366 to be a random process at local scales, but it is possible that combinations of factors cancel out to produce  
 367 seemingly random forest dynamics at large scales. In this case we should have observed power laws in a  
 368 limited set of situations that coincide with a critical point and we observed pervasive power law distributions  
 369 thus percolation is not the mechanisms that produce the observed distributions. This does not mean that  
 370 second order critical transitions are not present but that we can not detect them by means of patch size  
 371 distributions. The third mechanism suggested as the cause of pervasive power laws in patch size distribution  
 372 is facilitation (Irvine, Bull, & Keeling, 2016; Manor & Shnerb, 2008): a patch surrounded by forest will have  
 373 a smaller probability of been deforested or degraded than an isolated patch. We hypothesize that models  
 374 that include facilitation could explain the patterns observed here. The model of Scanlon et al. (2007) showed  
 375 an  $\alpha = 1.34$  which is different from our results (1.90 - 2.01 range). Another model but with three states  
 376 (tree/non-tree/degraded), including local facilitation and grazing, was also used to obtain power laws patch

377 distributions without external tuning, and exhibited deviations from power laws at high grazing pressures  
378 (S. Kéfi et al., 2007). The values of the power law exponent  $\alpha$  obtained for this model are dependent on the  
379 intensity of facilitation, when facilitation is more intense the exponent is higher, but the maximal values they  
380 obtained are still lower than the ones we observed. The interesting point is that the value of the exponent is  
381 dependent on the parameters, and thus the observed  $\alpha$  might be obtained with some parameter combination.

382 The existence of a critical transitions in forest, mainly in neotropical forest to savanna, is a matter of intense  
383 investigation, this is in general thought as first order or discontinuous transitions; we found power laws in  
384 forest patch distributions which is a necessary but not a sufficient condition for a second order or continuous  
385 transition. Moreover, a power law patch distribution can be indicative of a critical transition if it is present  
386 in a narrow range of conditions; conversely if it is not found, the existence of a critical transition cannot be  
387 discarded. Regardless this, new research suggested that first order transitions do not even exists when the  
388 system is spatially heterogeneous and present internal and external stochastic fluctuations as in forest; thus  
389 the application of indices based on second order transitions seems to be justified.

390 It has been suggested that a combination of spatial and temporal indicators could more reliably detect  
391 critical transitions (S. Kéfi et al., 2014). In this study, we combined five criteria to detect the closeness to  
392 a fragmentation threshold. Two of them were spatial: the forest patch size distribution, and the proportion  
393 of the largest patch relative to total forest area  $RS_{max}$ . The other three were the distribution of temporal  
394 fluctuations in the largest patch size, the trend in the variance, and the skewness of the fluctuations. One  
395 of them: the distribution of temporal fluctuations  $\Delta RS_{max}$  can not be applied with our temporal resolution  
396 due to the difficulties of fitting and comparing heavy tailed distributions. The combination of the remaining  
397 four gives us an increased degree of confidence about the system being close to a critical transition.

398 The monitoring of biggest patches using  $RS_{max}$  is also important regardless the existence or not of critical  
399 transitions.  $RS_{max}$  could be used to compare regions with different forest extension and as the total area  
400 of forest also change with different environmental condition is at least partially independent of climatic  
401 conditions could be also applied to compare forest from different latitudes. Moreover,  $RS_{max}$  contain most  
402 of the intact forest landscapes defined by P. Potapov et al. (2008), thus it is a relatively simple way to  
403 evaluate the risk in these areas.

404 We found that several continental areas and islands met our criteria, this analysis is at scale of continents so  
405 it is in fact a macrosystems perspective (Heffernan et al., 2014). In a macrosystems analysis it is important  
406 to link the local processes that produce the continental patterns, what we did here is to find the macro scale  
407 dynamical patterns that deserve attention. To link these patterns across scales requires a substantial amount

408 of investigation, probably performing the same analysis for smaller regions that identify more clearly which  
409 kind of forest and processes are locally involved. We know that the same procedure could be applied to local  
410 scales because the patch distributions are power laws; power law distributions are self-similar, or invariant  
411 to scale changes. Thus unless power law distribution are broken we could apply the same methodology to  
412 more local scales.

413 South America tropical and subtropical (SAST1), Southeast Asia mainland (SEAS1) and Africa mainland  
414 (AF1) met all criteria at least for one threshold; this regions experience the biggest rates of deforestation  
415 with a significant increase in loss of forest (M. C. Hansen et al., 2013). From our point of view the region  
416 most critical is the Southeast Asia because the proportion of the largest patch relative to total forest area  
417  $RS_{max}$  28%, then Africa with 33% and then South America with 56%. This is indicating that Southeast  
418 Asia is the most fragmented and thus the most endangered region. Due to the criteria we adopted to defined  
419 regions, we can not detect the effect of conservation policies applied at a country level, e.g. the Natural  
420 Forest Conservation Program in China, which produced an 1.6% increase in forest cover and net primary  
421 productivity (Viña, McConnell, Yang, Xu, & Liu, 2016).

422 Indonesia and Malaysia (OC3) both are countries with hight deforestation rates (M. C. Hansen et al., 2013);  
423 Sumatra (OC4) is the biggest island of Indonesia and where most deforestation occurs. Both regions show  
424 a high  $RS_{max}$  greater than 60% thus the forest is in an unfragmented state but they met all criteria, thus  
425 this means that they are approaching a transition if the actual deforestation rates continue. At present our  
426 indices are qualitative but we expect to develop them in a more quantitative way to predict how many years  
427 would be needed to complete a critical transition if actual forest loss rates are maintained.

428 The eurasian mainland region (EUAS1) is an extensive area with mainly temperate and boreal forest, and a  
429 combination of forest loss due to fire (P. Potapov, Hansen, Stehman, Loveland, & Pittman, 2008) and forestry.  
430 The biggest country is Russia that experienced the biggest rate of forest loss of all countries, but here in  
431 the zone of coniferous forest the the largest gain is observed due to agricultural abandonment (Prishchepov,  
432 Müller, Dubinin, Baumann, & Radeloff, 2013). The loss is maximum at the most dense areas of forest (M.  
433 C. Hansen et al., 2013, Table S3), this coincides with our analysis that detect an increasing risk at denser  
434 forest. This region also has a relatively low  $RS_{max}$  that means is probably near a fragmented state.

435 A region that is similar in forest composition to EAUS1 is North America (NA1); the two main countries  
436 involved, United States and Canada, are also in the first places of forest loss, with forest dynamics also  
437 mainly influenced by fire and forestry. Both regions are extensively managed for wood for industrial wood  
438 production, North America have a higher  $RS_{max}$  than eurasia and a positive skewness that excludes it from

439 beeing near a critical transition. A possible explanation of this is that in Russia after the collapse of the  
440 Soviet Union harvest was lower due to agricultural abandonment but illegal overharvesting of high valued  
441 stands increased (Gauthier, Bernier, Kuuluvainen, Shvidenko, & Schepaschenko, 2015) and that could be  
442 the cause of the differences we found between them.

443 The analysis of  $RS_{max}$  reveals that the island of Philippines (SEAS2) seems to be an example of a critical  
444 transition from an unconnected to a connected state, it can be qualitatively observed a transition from a state  
445 with high fluctuations and low  $RS_{max}$  to a state with low fluctuations and a high  $RS_{max}$ . If we observe this  
446 pattern backwards in time: the decrease in variance becomes and increase and negative skewness maintains  
447 the same, thus the region would show the criteria of a critical transition (Table 1, Figure S11). The actual  
448 pattern of transition to an unfragmented state could be the result of an active intervention of the government  
449 promoting conservation and rehabilitation of protected areas, ban of logging old-growth forest, reforestation  
450 of barren areas, community-based forestry activities, and sustainable forest management in the country's  
451 production forest (Lasco et al., 2008). This confirms that the early warning indicators proposed here work  
452 in the correct direction. The MODIS dataset does not detect if native forest is replaced by agroindustrial  
453 tree plantations like oil palms, that are among the main drivers of deforestation in this area (Malhi, Gardner,  
454 Goldsmith, Silman, & Zelazowski, 2014). To improve the estimation of forest patches, data sets as the  
455 MODIS cropland probability and others about land use, protected areas, forest type, should be incorporated  
456 (M. Hansen et al., 2014; J. O. Sexton et al., 2015).

457 Deforestation and fragmentation are closely related. At low levels of habitat reduction species population  
458 will decline proportionally; this can happen even when the habitat fragments retain connectivity. As habi-  
459 tation reduction continues, the critical threshold is approached and connectivity will have large fluctuations  
460 (Brook, Ellis, Perring, Mackay, & Blomqvist, 2013). This could trigger several negative synergistic effects:  
461 populations fluctuations and the possibility of extinctions will rise, increasing patch isolation and decreasing  
462 connectivity (Brook et al., 2013). This positive feedback mechanism will be enhanced when the fragmenta-  
463 tion threshold is reached, resulting in the loss of most habitat specialist species at a landscape scale (Pardini  
464 et al., 2010). Some authors argue that since species have heterogeneous responses to habitat loss and frag-  
465 mentation, and biotic dispersal is limited, the importance of thresholds is restricted to local scales or even  
466 that its existence is questionable (Brook et al., 2013). Fragmentation is by definition a local process that at  
467 some point produces emergent phenomena over the entire landscape, even if the area considered is infinite  
468 (B. Oborny, Meszéna, & Szabó, 2005). In addition, after a region's fragmentation threshold connectivity  
469 decreases, there is still a large and internally well connected patch that can maintain sensitive species (A. C.  
470 Martensen, Ribeiro, Banks-Leite, Prado, & Metzger, 2012). What is the time needed for these large patches

471 to become fragmented, and pose a real danger of extinction to a myriad of sensitive species? If a forest is  
472 already in a fragmented state, a second critical transition from forest to non-forest could happen, this was  
473 called the desertification transition (Corrado et al., 2014). Considering the actual trends of habitat loss,  
474 and studying the dynamics of non-forest patches—instead of the forest patches as we did here—the risk of  
475 this kind of transition could be estimated. The simple models proposed previously could also be used to  
476 estimate if these thresholds are likely to be continuous and reversible or discontinuous and often irreversible  
477 (Weissmann & Shnerb, 2016), and the degree of protection (e.g. using the set-asides strategy Banks-Leite et  
478 al. (2014)) than would be necessary to stop this trend.

479 The effectiveness of landscape management is related to the degree of fragmentation, and the criteria to  
480 direct reforestation efforts could be focused on regions near a transition (B. Oborny et al., 2007). Regions  
481 that are in an unconnected state require large efforts to recover a connected state, but regions that are near  
482 a transition could be easily pushed to a connected state; feedbacks due to facilitation mechanisms might  
483 help to maintain this state. Crossing the fragmentation critical point in forests could have negative effects  
484 on biodiversity and ecosystem services (Haddad et al., 2015), but it could also produce feedback loops at  
485 different levels of the biological hierarchy. This means that a critical transition produced at a continental  
486 scale could have effects at the level of communities, food webs, populations, phenotypes and genotypes  
487 (Barnosky et al., 2012). All these effects interact with climate change, thus there is a potential production of  
488 cascading effects that could lead to an abrupt climate change with potentially large ecological and economic  
489 impact (Alley et al., 2003).

490 Therefore, even if critical thresholds are reached only in some forest regions at a continental scale, a cascading  
491 effect with global consequences could still be produced, and may contribute to reach a planetary tipping point  
492 (Reyer, Rammig, Brouwers, & Langerwisch, 2015). The risk of such event will be higher if the dynamics of  
493 separate continental regions are coupled (Lenton & Williams, 2013). At least three of the regions defined  
494 here are considered tipping elements of the earth climate system that could be triggered during this century  
495 (Lenton et al., 2008). These were defined as policy relevant tipping elements so that political decisions could  
496 determine whether the critical value is reached or not. Thus using the criteria proposed here could be used  
497 as a more sensitive system to evaluate the closeness of a tipping point at a continental scale, but the same  
498 criteria could also be used to evaluate local problems at smaller areas. Further improvements will produce  
499 quantitative predictions about the temporal horizon where these critical transitions could produce significant  
500 changes in the studied systems.

501 **Supporting information**

502 **Appendix**

503 *Table S1:* Mean power-law exponent and Bootstrapped 95% confidence intervals by threshold.

504 *Table S2:* Mean power-law exponent and Bootstrapped 95% confidence intervals across thresholds by region  
505 and year.

506 *Table S3:* Mean total patch area; largest patch  $S_{max}$  in km<sup>2</sup>; largest patch proportional to total patch area  
507  $RS_{max}$  and 95% bootstrapped confidence interval of  $RS_{max}$ , by region and thresholds, averaged across years

508 *Table S4:* Model selection for distributions of fluctuation of largest patch  $\Delta S_{max}$  and largest patch relative  
509 to total forest area  $\Delta RS_{max}$ .

510 *Table S5:* Quantil regressions of the fluctuations of the largest patch vs year, for 10% and 90% quantils at  
511 different pixel thresholds.

512 *Table S6:* Unbiased estimation of Skewness of fluctuations of the largest patch  $\Delta S_{max}$  and fluctuations  
513 relative to total forest area  $\Delta RS_{max}$ .

514 *Figure S1:* Regions for Africa: Mainland (AF1), Madagascar (AF2).

515 *Figure S2:* Regions for Eurasia: Mainland (EUAS1), Japan (EUAS2), Great Britain (EUAS3).

516 *Figure S3:* Regions for North America: Mainland (NA1), Newfoundland (NA5).

517 *Figure S4:* Regions for Australia and islands: Australia mainland (OC1), New Guinea (OC2),  
518 Malaysia/Kalimantan (OC3), Sumatra (OC4), Sulawesi (OC5), New Zealand south island (OC6),  
519 Java (OC7), New Zealand north island (OC8).

520 *Figure S5:* Regions for South America: Tropical and subtropical forest up to Mexico (SAST1), Cuba  
521 (SAST2), South America Temperate forest (SAT1).

522 *Figure S6:* Regions for Southeast Asia: Mainland (SEAS1), Philippines (SEAS2).

523 *Figure S7:* Proportion of best models selected for patch size distributions using the Akaike criterion.

524 *Figure S8:* Power law exponents for forest patch distributions by year for all regions.

525 *Figure S9:* Average largest patch relative to total forest area  $RS_{max}$  by threshold, for all regions.

526 *Figure S10:* Largest patch relative to total forest area  $RS_{max}$  by year at 40% threshold, for regions with  
527 total forest area less than  $10^7$  km<sup>2</sup>.

528 *Figure S11*: Fluctuations of largest patch relative to total forest area  $RS_{max}$  for regions with total forest  
529 area less than  $10^7 \text{ km}^2$  by year and threshold.

530 **Data Accessibility**

531 Csv text file with model fits for patch size distribution, and model selection for all the regions; Gif Animations  
532 of a forest model percolation; Gif animations of largest patches; patch size files for all years and regions used  
533 here; and all the R, Python and Matlab scripts are available at figshare [http://dx.doi.org/10.6084/m9.  
534 figshare.4263905](http://dx.doi.org/10.6084/m9.figshare.4263905).

535 **Acknowledgments**

536 LAS and SRD are grateful to the National University of General Sarmiento for financial support. We want to  
537 thank to Jordi Bascompte, Nara Guisoni, Fernando Momo, and two anonymous reviewers for their comments  
538 and discussions that greatly improved the manuscript. This work was partially supported by a grant from  
539 CONICET (PIO 144-20140100035-CO).

540 **References**

- 541 Alley, R. B., Marotzke, J., Nordhaus, W. D., Overpeck, J. T., Peteet, D. M., Pielke, R. A., ... Wallace, J. M.  
542 (2003). Abrupt Climate Change. *Science*, 299(5615), 2005–2010. Retrieved from <http://science.sciencemag.org/content/299/5615/2005.abstract>
- 543 Allington, G. R. H., & Valone, T. J. (2010). Reversal of desertification: The role of physical and chemical  
544 soil properties. *Journal of Arid Environments*, 74(8), 973–977. doi:10.1016/j.jaridenv.2009.12.005
- 545 Alstott, J., Bullmore, E., & Plenz, D. (2014). powerlaw: A Python Package for Analysis of Heavy-Tailed  
546 Distributions. *PLOS ONE*, 9(1), e85777. Retrieved from <https://doi.org/10.1371/journal.pone.0085777>
- 547 Angelsen, A. (2010). Policies for reduced deforestation and their impact on agricultural production. *Proceedings of the National Academy of Sciences*, 107(46), 19639–19644. doi:10.1073/pnas.0912014107
- 548 Banks-Leite, C., Pardini, R., Tambosi, L. R., Pearse, W. D., Bueno, A. A., Bruscagin, R. T., ... Metzger,  
549 J. P. (2014). Using ecological thresholds to evaluate the costs and benefits of set-asides in a biodiversity  
550 hotspot. *Science*, 345(6200), 1041–1045. doi:10.1126/science.1255768
- 551 Barnosky, A. D., Hadly, E. A., Bascompte, J., Berlow, E. L., Brown, J. H., Fortelius, M., ... Smith, A. B.

- 554 (2012). Approaching a state shift in Earth's biosphere. *Nature*, 486(7401), 52–58. doi:10.1038/nature11018
- 555 Bascompte, J., & Solé, R. V. (1996). Habitat fragmentation and extinction thresholds in spatially explicit  
556 models. *Journal of Animal Ecology*, 65(4), 465–473. doi:10.2307/5781
- 557 Bazant, M. Z. (2000). Largest cluster in subcritical percolation. *Physical Review E*, 62(2), 1660–1669.  
558 Retrieved from <http://link.aps.org/doi/10.1103/PhysRevE.62.1660>
- 559 Belward, A. S. (1996). *The IGBP-DIS Global 1 Km Land Cover Data Set "DISCover": Proposal and  
560 Implementation Plans : Report of the Land Recover Working Group of IGBP-DIS* (p. 61). IGBP-DIS Office.  
561 Retrieved from <https://books.google.com.ar/books?id=qixsNAAACAAJ>
- 562 Benedetti-Cecchi, L., Tamburello, L., Maggi, E., & Bulleri, F. (2015). Experimental Perturbations Mod-  
563 ify the Performance of Early Warning Indicators of Regime Shift. *Current Biology*, 25(14), 1867–1872.  
564 doi:10.1016/j.cub.2015.05.035
- 565 Bestelmeyer, B. T., Duniway, M. C., James, D. K., Burkett, L. M., & Havstad, K. M. (2013). A test of  
566 critical thresholds and their indicators in a desertification-prone ecosystem: more resilience than we thought.  
567 *Ecology Letters*, 16, 339–345. doi:10.1111/ele.12045
- 568 Bestelmeyer, B. T., Ellison, A. M., Fraser, W. R., Gorman, K. B., Holbrook, S. J., Laney, C. M., ... Sharma,  
569 S. (2011). Analysis of abrupt transitions in ecological systems. *Ecosphere*, 2(12), 129. doi:10.1890/ES11-  
570 00216.1
- 571 Boettiger, C., & Hastings, A. (2012). Quantifying limits to detection of early warning for critical transitions.  
572 *Journal of the Royal Society Interface*, 9(75), 2527–2539. doi:10.1098/rsif.2012.0125
- 573 Bonan, G. B. (2008). Forests and Climate Change: Forcings, Feedbacks, and the Climate Benefits of Forests.  
574 *Science*, 320(5882), 1444–1449. doi:10.1126/science.1155121
- 575 Botet, R., & Ploszajczak, M. (2004). Correlations in Finite Systems and Their Universal Scaling Properties.  
576 In K. Morawetz (Ed.), *Nonequilibrium physics at short time scales: Formation of correlations* (pp. 445–466).  
577 Berlin Heidelberg: Springer-Verlag.
- 578 Brook, B. W., Ellis, E. C., Perring, M. P., Mackay, A. W., & Blomqvist, L. (2013). Does the terrestrial  
579 biosphere have planetary tipping points? *Trends in Ecology & Evolution*. doi:10.1016/j.tree.2013.01.016
- 580 Burnham, K., & Anderson, D. R. (2002). *Model selection and multi-model inference: A practical information-  
581 theoretic approach* (2nd. ed., p. 512). New York: Springer-Verlag.
- 582 Canfield, D. E., Glazer, A. N., & Falkowski, P. G. (2010). The Evolution and Future of Earth's Nitrogen

- 583 Cycle. *Science*, 330(6001), 192–196. doi:10.1126/science.1186120
- 584 Carpenter, S. R., Cole, J. J., Pace, M. L., Batt, R., Brock, W. A., Cline, T., ... Weidel, B. (2011).  
585 Early Warnings of Regime Shifts: A Whole-Ecosystem Experiment. *Science*, 332(6033), 1079–1082.  
586 doi:10.1126/science.1203672
- 587 Clauset, A., Shalizi, C., & Newman, M. (2009). Power-Law Distributions in Empirical Data. *SIAM Review*,  
588 51(4), 661–703. doi:10.1137/070710111
- 589 Corrado, R., Cherubini, A. M., & Pennetta, C. (2014). Early warning signals of desertification transitions  
590 in semiarid ecosystems. *Physical Review E - Statistical, Nonlinear, and Soft Matter Physics*, 90(6), 62705.  
591 doi:10.1103/PhysRevE.90.062705
- 592 Crawley, M. J. (2012). *The R Book* (2nd. ed., p. 1076). Hoboken, NJ, USA: Wiley.
- 593 Crowther, T. W., Glick, H. B., Covey, K. R., Bettigole, C., Maynard, D. S., Thomas, S. M., ... Bradford, M.  
594 A. (2015). Mapping tree density at a global scale. *Nature*, 525(7568), 201–205. doi:10.1038/nature14967
- 595 Dai, L., Vorselen, D., Korolev, K. S., & Gore, J. (2012). Generic Indicators for Loss of Resilience Before a  
596 Tipping Point Leading to Population Collapse. *Science*, 336(6085), 1175–1177. doi:10.1126/science.1219805
- 597 DiMiceli, C., Carroll, M., Sohlberg, R., Huang, C., Hansen, M., & Townshend, J. (2015). Annual Global Au-  
598 tomated MODIS Vegetation Continuous Fields (MOD44B) at 250 m Spatial Resolution for Data Years Begin-  
599 ning Day 65, 2000 - 2014, Collection 051 Percent Tree Cover, University of Maryland, College Park, MD, USA.  
600 Retrieved from [https://lpdaac.usgs.gov/dataset{\\\_}discovery/modis/modis{\\\_}products{\\\_}table/mod44b](https://lpdaac.usgs.gov/dataset{\_}discovery/modis/modis{\_}products{\_}table/mod44b)
- 601 Drake, J. M., & Griffen, B. D. (2010). Early warning signals of extinction in deteriorating environments.  
602 *Nature*, 467(7314), 456–459. doi:10.1038/nature09389
- 603 Efron, B., & Tibshirani, R. J. (1994). *An Introduction to the Bootstrap* (p. 456). New York: Taylor &  
604 Francis. Retrieved from <https://books.google.es/books?id=gLlpIUXRntoC>
- 605 Filotas, E., Parrott, L., Burton, P. J., Chazdon, R. L., Coates, K. D., Coll, L., ... Messier, C. (2014). Viewing  
606 forests through the lens of complex systems science. *Ecosphere*, 5(January), 1–23. doi:10.1890/ES13-00182.1
- 607 Foley, J. A., Ramankutty, N., Brauman, K. A., Cassidy, E. S., Gerber, J. S., Johnston, M., ... Zaks, D. P. M.  
608 (2011). Solutions for a cultivated planet. *Nature*, 478(7369), 337–342. doi:10.1038/nature10452
- 609 Folke, C., Jansson, Å., Rockström, J., Olsson, P., Carpenter, S. R., Iii, F. S. C., ... Westley, F. (2011).  
610 Reconnecting to the Biosphere. *AMBIO*, 40(7), 719–738. doi:10.1007/s13280-011-0184-y
- 611 Fung, T., O'Dwyer, J. P., Rahman, K. A., Fletcher, C. D., & Chisholm, R. A. (2016). Reproducing static

- 612 and dynamic biodiversity patterns in tropical forests: the critical role of environmental variance. *Ecology*,  
613 97(5), 1207–1217. doi:10.1890/15-0984.1
- 614 Gardner, R. H., & Urban, D. L. (2007). Neutral models for testing landscape hypotheses. *Landscape Ecology*,  
615 22(1), 15–29. doi:10.1007/s10980-006-9011-4
- 616 Gastner, M. T., Oborny, B., Zimmermann, D. K., & Pruessner, G. (2009). Transition from Connected  
617 to Fragmented Vegetation across an Environmental Gradient: Scaling Laws in Ecotone Geometry. *The*  
618 *American Naturalist*, 174(1), E23–E39. doi:10.1086/599292
- 619 Gauthier, S., Bernier, P., Kuuluvainen, T., Shvidenko, A. Z., & Schepaschenko, D. G. (2015). Boreal forest  
620 health and global change. *Science*, 349(6250), 819 LP–822. Retrieved from <http://science.sciencemag.org/>  
621 content/349/6250/819.abstract
- 622 Gilman, S. E., Urban, M. C., Tewksbury, J., Gilchrist, G. W., & Holt, R. D. (2010). A framework  
623 for community interactions under climate change. *Trends in Ecology & Evolution*, 25(6), 325–331.  
624 doi:10.1016/j.tree.2010.03.002
- 625 Goldstein, M. L., Morris, S. A., & Yen, G. G. (2004). Problems with fitting to the power-law distri-  
626 bution. *The European Physical Journal B - Condensed Matter and Complex Systems*, 41(2), 255–258.  
627 doi:10.1140/epjb/e2004-00316-5
- 628 Haddad, N. M., Brudvig, L. a., Clobert, J., Davies, K. F., Gonzalez, A., Holt, R. D., ... Townshend, J. R.  
629 (2015). Habitat fragmentation and its lasting impact on Earth's ecosystems. *Science Advances*, 1(2), 1–9.  
630 doi:10.1126/sciadv.1500052
- 631 Hansen, M. C., Potapov, P. V., Moore, R., Hancher, M., Turubanova, S. A., Tyukavina, A., ... Townshend,  
632 J. R. G. (2013). High-Resolution Global Maps of 21st-Century Forest Cover Change. *Science*, 342(6160),  
633 850–853. doi:10.1126/science.1244693
- 634 Hansen, M., Potapov, P., Margono, B., Stehman, S., Turubanova, S., & Tyukavina, A. (2014). Response  
635 to Comment on “High-resolution global maps of 21st-century forest cover change”. *Science*, 344(6187), 981.  
636 doi:10.1126/science.1248817
- 637 Hantson, S., Pueyo, S., & Chuvieco, E. (2015). Global fire size distribution is driven by human impact and  
638 climate. *Global Ecology and Biogeography*, 24(1), 77–86. doi:10.1111/geb.12246
- 639 Harris, T. E. (1974). Contact interactions on a lattice. *The Annals of Probability*, 2, 969–988.
- 640 Hartigan, J. A., & Hartigan, P. M. (1985). The Dip Test of Unimodality. *The Annals of Statistics*, 13(1),

- 641 70–84. Retrieved from <http://www.jstor.org/stable/2241144>
- 642 Hastings, A., & Wysham, D. B. (2010). Regime shifts in ecological systems can occur with no warning.
- 643 *Ecology Letters*, 13(4), 464–472. doi:10.1111/j.1461-0248.2010.01439.x
- 644 He, F., & Hubbell, S. (2003). Percolation Theory for the Distribution and Abundance of Species. *Physical*
- 645 *Review Letters*, 91(19), 198103. doi:10.1103/PhysRevLett.91.198103
- 646 Heffernan, J. B., Soranno, P. A., Angilletta, M. J., Buckley, L. B., Gruner, D. S., Keitt, T. H., ... Weathers,
- 647 K. C. (2014). Macrosystems ecology: understanding ecological patterns and processes at continental scales.
- 648 *Frontiers in Ecology and the Environment*, 12(1), 5–14. doi:10.1890/130017
- 649 Hinrichsen, H. (2000). Non-equilibrium critical phenomena and phase transitions into absorbing states.
- 650 *Advances in Physics*, 49(7), 815–958. doi:10.1080/00018730050198152
- 651 Hirota, M., Holmgren, M., Nes, E. H. V., & Scheffer, M. (2011). Global Resilience of Tropical Forest and
- 652 Savanna to Critical Transitions. *Science*, 334(6053), 232–235. doi:10.1126/science.1210657
- 653 Irvine, M. A., Bull, J. C., & Keeling, M. J. (2016). Aggregation dynamics explain vegetation patch-size
- 654 distributions. *Theoretical Population Biology*, 108, 70–74. doi:10.1016/j.tpb.2015.12.001
- 655 Keitt, T. H., Urban, D. L., & Milne, B. T. (1997). Detecting critical scales in fragmented landscapes.
- 656 *Conservation Ecology*, 1(1), 4. Retrieved from <http://www.ecologyandsociety.org/vol1/iss1/art4/>
- 657 Kéfi, S., Guttal, V., Brock, W. A., Carpenter, S. R., Ellison, A. M., Livina, V. N., ... Dakos, V. (2014).
- 658 Early Warning Signals of Ecological Transitions: Methods for Spatial Patterns. *PLoS ONE*, 9(3), e92097.
- 659 doi:10.1371/journal.pone.0092097
- 660 Kéfi, S., Rietkerk, M., Alados, C. L., Pueyo, Y., Papanastasis, V. P., ElAich, A., & Ruiter, P. C. de.
- 661 (2007). Spatial vegetation patterns and imminent desertification in Mediterranean arid ecosystems. *Nature*,
- 662 449(7159), 213–217. doi:10.1038/nature06111
- 663 Kitzberger, T., Aráoz, E., Gowda, J. H., Mermoz, M., & Morales, J. M. (2012). Decreases in Fire Spread
- 664 Probability with Forest Age Promotes Alternative Community States, Reduced Resilience to Climate Vari-
- 665 ability and Large Fire Regime Shifts. *Ecosystems*, 15(1), 97–112. doi:10.1007/s10021-011-9494-y
- 666 Koenker, R. (2016). quantreg: Quantile Regression. Retrieved from <http://cran.r-project.org/package=quantreg>
- 668 Lasco, R. D., Pulhin, F. B., Cruz, R. V. O., Pulhin, J. M., Roy, S. S. N., & Sanchez, P. A. J. (2008). Forest
- 669 responses to changing rainfall in the Philippines. In N. Leary, C. Conde, & J. Kulkarni (Eds.), *Climate*

- 670 change and vulnerability (pp. 49–66). London: Earthscan. Retrieved from <http://gen.lib.rus.ec/book/index.php?md5=AD313B13E05C9D61A9EC1EE2E73A91FB>
- 671
- 672 Leibold, M. A., & Norberg, J. (2004). Biodiversity in metacommunities: Plankton as complex adaptive  
673 systems? *Limnology and Oceanography*, 49(4, part 2), 1278–1289. doi:10.4319/lo.2004.49.4\_part\_2.1278
- 674 Lenton, T. M., & Williams, H. T. P. (2013). On the origin of planetary-scale tipping points. *Trends in  
675 Ecology & Evolution*, 28(7), 380–382. doi:10.1016/j.tree.2013.06.001
- 676 Lenton, T. M., Held, H., Kriegler, E., Hall, J. W., Lucht, W., Rahmstorf, S., & Schellnhuber, H. J. (2008).  
677 Tipping elements in the Earth's climate system. *Proceedings of the National Academy of Sciences*, 105(6),  
678 1786–1793. doi:10.1073/pnas.0705414105
- 679 Limpert, E., Stahel, W. A., & Abbt, M. (2001). Log-normal Distributions across the Sciences: Keys and  
680 CluesOn the charms of statistics, and how mechanical models resembling gambling machines offer a link to  
681 a handy way to characterize log-normal distributions, which can provide deeper insight into var. *BioScience*,  
682 51(5), 341–352. Retrieved from [http://dx.doi.org/10.1641/0006-3568\(2001\)051\[0341:LNDATS\]2.0.CO](http://dx.doi.org/10.1641/0006-3568(2001)051[0341:LNDATS]2.0.CO)
- 683 Loehle, C., Li, B.-L., & Sundell, R. C. (1996). Forest spread and phase transitions at forest-prairie ecotones  
684 in Kansas, U.S.A. *Landscape Ecology*, 11(4), 225–235.
- 685 Malhi, Y., Gardner, T. A., Goldsmith, G. R., Silman, M. R., & Zelazowski, P. (2014). Tropical Forests in  
686 the Anthropocene. *Annual Review of Environment and Resources*, 39(1), 125–159. doi:10.1146/annurev-  
687 environ-030713-155141
- 688 Manor, A., & Shnerb, N. M. (2008). Origin of pareto-like spatial distributions in ecosystems. *Physical  
689 Review Letters*, 101(26), 268104. doi:10.1103/PhysRevLett.101.268104
- 690 Martensen, A. C., Ribeiro, M. C., Banks-Leite, C., Prado, P. I., & Metzger, J. P. (2012). Associations  
691 of Forest Cover, Fragment Area, and Connectivity with Neotropical Understory Bird Species Richness and  
692 Abundance. *Conservation Biology*, 26(6), 1100–1111. doi:10.1111/j.1523-1739.2012.01940.x
- 693 McKenzie, D., & Kennedy, M. C. (2012). Power laws reveal phase transitions in landscape con-  
694 trols of fire regimes. *Nat Commun*, 3, 726. Retrieved from <http://dx.doi.org/10.1038/ncomms1731>  
695 [http://www.nature.com/ncomms/journal/v3/n3/supplinfo/ncomms1731{\\\_\}S1.html](http://www.nature.com/ncomms/journal/v3/n3/supplinfo/ncomms1731{\_\}S1.html)
- 696 Mitchell, M. G. E., Suarez-Castro, A. F., Martinez-Harms, M., Maron, M., McAlpine, C., Gaston, K. J., ...  
697 Rhodes, J. R. (2015). Reframing landscape fragmentation's effects on ecosystem services. *Trends in Ecology*

- 698 & *Evolution*, 30(4), 190–198. doi:10.1016/j.tree.2015.01.011
- 699 Naito, A. T., & Cairns, D. M. (2015). Patterns of shrub expansion in Alaskan arctic river corridors suggest  
700 phase transition. *Ecology and Evolution*, 5(1), 87–101. doi:10.1002/ece3.1341
- 701 Newman, M. E. J. (2005). Power laws, Pareto distributions and Zipf's law. *Contemporary Physics*, 46(5),  
702 323–351. doi:10.1080/00107510500052444
- 703 Oborny, B., Meszéna, G., & Szabó, G. (2005). Dynamics of Populations on the Verge of Extinction. *Oikos*,  
704 109(2), 291–296. Retrieved from <http://www.jstor.org/stable/3548746>
- 705 Oborny, B., Szabó, G., & Meszéna, G. (2007). Survival of species in patchy landscapes: percolation in  
706 space and time. In *Scaling biodiversity* (pp. 409–440). Cambridge University Press. Retrieved from <http://dx.doi.org/10.1017/CBO9780511814938.022>
- 708 Ochoa-Quintero, J. M., Gardner, T. A., Rosa, I., de Barros Ferraz, S. F., & Sutherland, W. J. (2015).  
709 Thresholds of species loss in Amazonian deforestation frontier landscapes. *Conservation Biology*, 29(2),  
710 440–451. doi:10.1111/cobi.12446
- 711 Ódor, G. (2004). Universality classes in nonequilibrium lattice systems. *Reviews of Modern Physics*, 76(3  
712 I), 663–724. doi:10.1103/RevModPhys.76.663
- 713 Pardini, R., Bueno, A. de A., Gardner, T. A., Prado, P. I., & Metzger, J. P. (2010). Beyond the Fragmen-  
714 tation Threshold Hypothesis: Regime Shifts in Biodiversity Across Fragmented Landscapes. *PLoS ONE*,  
715 5(10), e13666. doi:10.1371/journal.pone.0013666
- 716 Potapov, P., Hansen, M. C., Stehman, S. V., Loveland, T. R., & Pittman, K. (2008). Combining MODIS  
717 and Landsat imagery to estimate and map boreal forest cover loss. *Remote Sensing of Environment*, 112(9),  
718 3708–3719. doi:<https://doi.org/10.1016/j.rse.2008.05.006>
- 719 Potapov, P., Yaroshenko, A., Turubanova, S., Dubinin, M., Laestadius, L., Thies, C., ... Zhuravleva, I. (2008).  
720 Mapping the world's intact forest landscapes by remote sensing. *Ecology and Society*, 13(2).
- 721 Prishchepov, A. V., Müller, D., Dubinin, M., Baumann, M., & Radeloff, V. C. (2013). Determinants  
722 of agricultural land abandonment in post-Soviet European Russia. *Land Use Policy*, 30(1), 873–884.  
723 doi:<https://doi.org/10.1016/j.landusepol.2012.06.011>
- 724 Pueyo, S., de Alencastro Graça, P. M. L., Barbosa, R. I., Cots, R., Cardona, E., & Fearnside, P. M. (2010).  
725 Testing for criticality in ecosystem dynamics: the case of Amazonian rainforest and savanna fire. *Ecology*

- 726 *Letters*, 13(7), 793–802. doi:10.1111/j.1461-0248.2010.01497.x
- 727 R Core Team. (2015). R: A Language and Environment for Statistical Computing. Vienna, Austria: R  
728 Foundation for Statistical Computing. Retrieved from <http://www.r-project.org/>
- 729 Reyer, C. P. O., Rammig, A., Brouwers, N., & Langerwisch, F. (2015). Forest resilience, tipping points and  
730 global change processes. *Journal of Ecology*, 103(1), 1–4. doi:10.1111/1365-2745.12342
- 731 Rockstrom, J., Steffen, W., Noone, K., Persson, A., Chapin, F. S., Lambin, E. F., ... Foley, J. A. (2009). A  
732 safe operating space for humanity. *Nature*, 461(7263), 472–475. Retrieved from <http://dx.doi.org/10.1038/461472a>
- 733
- 734 Rooij, M. M. J. W. van, Nash, B., Rajaraman, S., & Holden, J. G. (2013). A Fractal Approach to Dynamic  
735 Inference and Distribution Analysis. *Frontiers in Physiology*, 4(1). doi:10.3389/fphys.2013.00001
- 736 Rudel, T. K., Coomes, O. T., Moran, E., Achard, F., Angelsen, A., Xu, J., & Lambin, E. (2005). Forest  
737 transitions: towards a global understanding of land use change. *Global Environmental Change*, 15(1), 23–31.  
738 doi:<https://doi.org/10.1016/j.gloenvcha.2004.11.001>
- 739 Saravia, L. A., & Momo, F. R. (2017). Biodiversity collapse and early warning indicators in  
740 a spatial phase transition between neutral and niche communities. *PeerJ PrePrints*, 5, e1589v4.  
741 doi:10.7287/peerj.preprints.1589v3
- 742 Scanlon, T. M., Caylor, K. K., Levin, S. A., & Rodriguez-iturbe, I. (2007). Positive feedbacks promote  
743 power-law clustering of Kalahari vegetation. *Nature*, 449(September), 209–212. doi:10.1038/nature06060
- 744 Scheffer, M., Bascompte, J., Brock, W. A., Brovkin, V., Carpenter, S. R., Dakos, V., ... Sugihara, G. (2009).  
745 Early-warning signals for critical transitions. *Nature*, 461(7260), 53–59. doi:10.1038/nature08227
- 746 Scheffer, M., Walker, B., Carpenter, S., Foley, J. a, Folke, C., & Walker, B. (2001). Catastrophic shifts in  
747 ecosystems. *Nature*, 413(6856), 591–596. doi:10.1038/35098000
- 748 Seidler, T. G., & Plotkin, J. B. (2006). Seed Dispersal and Spatial Pattern in Tropical Trees. *PLoS Biology*,  
749 4(11), e344. doi:10.1371/journal.pbio.0040344
- 750 Sexton, J. O., Noojipady, P., Song, X.-P., Feng, M., Song, D.-X., Kim, D.-H., ... Townshend, J. R.  
751 (2015). Conservation policy and the measurement of forests. *Nature Climate Change*, 6(2), 192–196.  
752 doi:10.1038/nclimate2816
- 753 Sexton, J. O., Song, X.-P., Feng, M., Noojipady, P., Anand, A., Huang, C., ... Townshend, J. R. (2013).  
754 Global, 30-m resolution continuous fields of tree cover: Landsat-based rescaling of MODIS vegetation con-

- 755 tinuous fields with lidar-based estimates of error. *International Journal of Digital Earth*, 6(5), 427–448.
- 756 doi:10.1080/17538947.2013.786146
- 757 Solé, R. V. (2011). *Phase Transitions* (p. 223). Princeton University Press. Retrieved from <https://books.google.com.ar/books?id=8RcLuv-Ll2kC>
- 759 Solé, R. V., & Bascompte, J. (2006). *Self-organization in complex ecosystems* (p. 373). New Jersey, USA.:  
760 Princeton University Press. Retrieved from <http://books.google.com.ar/books?id=v4gpGH6Gv68C>
- 761 Solé, R. V., Alonso, D., & Mckane, A. (2002). Self-organized instability in complex ecosystems. *Philoso-  
762 sophical Transactions of the Royal Society of London. Series B, Biological Sciences*, 357(May), 667–681.  
763 doi:10.1098/rstb.2001.0992
- 764 Solé, R. V., Alonso, D., & Saldaña, J. (2004). Habitat fragmentation and biodiversity collapse in neutral  
765 communities. *Ecological Complexity*, 1(1), 65–75. doi:10.1016/j.ecocom.2003.12.003
- 766 Solé, R. V., Bartumeus, F., & Gamarra, J. G. P. (2005). Gap percolation in rainforests. *Oikos*, 110(1),  
767 177–185. doi:10.1111/j.0030-1299.2005.13843.x
- 768 Staal, A., Dekker, S. C., Xu, C., & Nes, E. H. van. (2016). Bistability, Spatial Interaction, and the  
769 Distribution of Tropical Forests and Savannas. *Ecosystems*, 19(6), 1080–1091. doi:10.1007/s10021-016-0011-  
770 1
- 771 Stauffer, D., & Aharony, A. (1994). *Introduction To Percolation Theory* (p. 179). London: Taylor & Francis.
- 772 Vasilakopoulos, P., & Marshall, C. T. (2015). Resilience and tipping points of an exploited fish population  
773 over six decades. *Global Change Biology*, 21(5), 1834–1847. doi:10.1111/gcb.12845
- 774 Verbesselt, J., Umlauf, N., Hirota, M., Holmgren, M., Van Nes, E. H., Herold, M., ... Scheffer, M. (2016). Re-  
775 motely sensed resilience of tropical forests. *Nature Climate Change*, 1(September). doi:10.1038/nclimate3108
- 776 Villa Martín, P., Bonachela, J. A., & Muñoz, M. A. (2014). Quenched disorder forbids discontinuous  
777 transitions in nonequilibrium low-dimensional systems. *Physical Review E*, 89(1), 12145. Retrieved from  
778 <https://link.aps.org/doi/10.1103/PhysRevE.89.012145>
- 779 Villa Martín, P., Bonachela, J. A., Levin, S. A., & Muñoz, M. A. (2015). Eluding catastrophic shifts.  
780 *Proceedings of the National Academy of Sciences*, 112(15), E1828–E1836. doi:10.1073/pnas.1414708112
- 781 Viña, A., McConnell, W. J., Yang, H., Xu, Z., & Liu, J. (2016). Effects of conservation policy on China's  
782 forest recovery. *Science Advances*, 2(3), e1500965. Retrieved from <http://advances.sciencemag.org/content/>

783 2/3/e1500965.abstract

- 784 Vuong, Q. H. (1989). Likelihood Ratio Tests for Model Selection and Non-Nested Hypotheses. *Econometrica*,  
785 57(2), 307–333. doi:10.2307/1912557
- 786 Weerman, E. J., Van Belzen, J., Rietkerk, M., Temmerman, S., Kéfi, S., Herman, P. M. J., & Koppell, J. V.  
787 de. (2012). Changes in diatom patch-size distribution and degradation in a spatially self-organized intertidal  
788 mudflat ecosystem. *Ecology*, 93(3), 608–618. doi:10.1890/11-0625.1
- 789 Weissmann, H., & Shnerb, N. M. (2016). Predicting catastrophic shifts. *Journal of Theoretical Biology*, 397,  
790 128–134. doi:10.1016/j.jtbi.2016.02.033
- 791 Wuyts, B., Champneys, A. R., & House, J. I. (2017). Amazonian forest-savanna bistability and human  
792 impact. *Nature Communications*, 8(May), 15519. doi:10.1038/ncomms15519
- 793 Xu, C., Hantson, S., Holmgren, M., Nes, E. H. van, Staal, A., & Scheffer, M. (2016). Remotely sensed  
794 canopy height reveals three pantropical ecosystem states. *Ecology*, 97(9), 2518–2521. doi:10.1002/ecy.1470
- 795 Zhang, J. Y., Wang, Y., Zhao, X., Xie, G., & Zhang, T. (2005). Grassland recovery by protection from  
796 grazing in a semi-arid sandy region of northern China. *New Zealand Journal of Agricultural Research*, 48(2),  
797 277–284. doi:10.1080/00288233.2005.9513657
- 798 Zinck, R. D., & Grimm, V. (2009). Unifying wildfire models from ecology and statistical physics. *The  
799 American Naturalist*, 174(5), E170–85. doi:10.1086/605959